Novel Selective Inhibitors of Neutral Endopeptidase for the Treatment of Female Sexual Arousal Disorder. Synthesis and Activity of Functionalized Glutaramides

David C. Pryde,*,† Graham N. Maw,† Simon Planken,† Michelle Y. Platts,† Vivienne Sanderson,† Martin Corless,† Alan Stobie,† Christopher G. Barber,‡ Rachel Russell,‡ Laura Foster,‡ Laura Barker,‡ Christopher Wayman,‡ Piet Van Der Graaf,‡ Peter Stacey,‡ Debbie Morren,‡ Christopher Kohl,§ Kevin Beaumont,§ Sara Coggon,§ and Michael Tute||

Departments of Discovery Chemistry, Discovery Biology, Pharmacokinetics, Dynamics and Metabolism, and Molecular Informatics and Structure Based Design, Pfizer Global Research and Development, Sandwich, Kent CT13 9NJ, U.K.

Received February 7, 2006

Female sexual arousal disorder (FSAD) is a highly prevalent sexual disorder affecting up to 40% of women. We describe herein our efforts to identify a selective neutral endopeptidase (NEP) inhibitor as a potential treatment for FSAD. The rationale for this approach, together with a description of the medicinal chemistry strategy, lead compounds, and SAR investigations are detailed. In particular, the strategy of starting with the clinically precedented selective NEP inhibitor, Candoxatrilat, and targeting low molecular weight and relatively polar mono-carboxylic acids is described. This led ultimately to the prototype development candidate *R*-**13**, for which detailed pharmacology and pharmacokinetic parameters are presented.[1]

Introduction

Female sexual dysfunction (FSD)[a] is the difficulty or inability of a woman to find satisfaction in sexual expression and is a collective term for several diverse disorders including female sexual arousal disorder (FSAD), desire disorder, and painful intercourse disorder. FSAD is "a persistent or recurrent inability to attain or to maintain until completion of the sexual activity adequate lubrication-swelling response of sexual excitement".[2] There are wide variations in the reported incidence and prevalence of FSAD, partly because of differing evaluation criteria, but most investigators report a higher incidence of arousal disorders in otherwise healthy women than they do erectile dysfunction in the male population. It is therefore a highly prevalent disorder within females, affecting up to 40% of pre, peri, and postmenopausal women[3] and is often accompanied by concomitant complaints such as an inability to achieve orgasm and depression. Current therapies for treating FSAD are limited to psychological counselling, over-the-counter sexual lubricants, and several investigational candidates such as hormonal agents and drug candidates approved for other conditions such as male erectile dysfunction.

It has been proposed that the most common cause of FSAD is decreased genital blood flow resulting in reduced vaginal, labial, and clitoral engorgement.[4] Vasoactive intestinal peptide (VIP) is an endogenous vasodilator thought to have a key role in the control of vaginal blood flow,[5] its action being mediated by cyclic AMP. The blood vessels supplying the vagina are densely innervated by VIP-containing neurones. VIP is a 28 amino acid peptide, which is rapidly degraded in the liver, and is unsuitable for oral dosing as a therapy for FSAD. It is known that VIP is degraded by endogenous neutral endopeptidase (NEP, EC3.4.24.11), and it was our hypothesis that by selectively inhibiting NEP, one could potentiate VIP levels and thereby enhance VIP-induced increases in vaginal blood flow. There are many inhibitors of NEP known in the literature,[6] many of which inhibit both NEP and the related enzyme, angiotensin converting enzyme (ACE)[7] with accompanying influence on cardiovascular parameters. This highlighted ACE as a key selectivity target to avoid any significant vasodilatory effects in this nonlife-threatening condition. The most advanced example of a selective NEP inhibitor is Candoxatril,[8] a 5-indanyl ester prodrug of the active constituent Candoxatrilat **1**, which was progressed into clinical trials in the 1990s for chronic heart failure. Because **1** had already successfully completed a preclinical toxicology program, had a proven benign pharmacological profile in humans, represented a Pfizer proprietary chemical series, and was a well-precedented chemotype, we chose this as our starting point.

In targeting a *prn* treatment for FSAD, we sought a relatively short half-life ($T_{1/2}$ < 10 h), rapid onset (T_{max} < 1 h) potent inhibitor of NEP. Ideally, the target agent would not require derivatization as a prodrug, simplifying its pharmacokinetic profile and preclinical development, but rather the parent drug would be completely absorbed and demonstrate high bioavailability. This effectively ruled out the use of Candoxatril itself for this program. Our strategy was to target a potent monocarboxylic acid based around the glutaramide template of Candoxatrilat by removing the non-Zn-binding carboxylic acid in (**1**) and optimizing the amide substituent. This strategy is depicted in the Figure 1. Modification of the amide substituent X would allow the potency and physicochemistry to be easily probed. A late-stage amide-forming step would also be amenable to parallel synthesis techniques, greatly expediting SAR generation. Further fine-tuning of the physical properties could be provided by changes to the P_1' side chain grouping Y.

By combining small groups X and Y, a substantial number of potent NEP inhibitors were accessed relatively quickly, all of which showed excellent selectivity (>300-fold) over related zinc-metalloproteases, such as ACE and the related endothelin converting enzyme (ECE). The synthesis and structure−activity

* Corresponding author. Tel: (01304) 616161. Fax: (01304) 651819. E-mail: David.Pryde@pfizer.com.
† Department of Discovery Chemistry.
‡ Department of Discovery Biology.
§ Department of Pharmacokinetics, Dynamics and Metabolism.
|| Department of Molecular Informatics and Structure Based Design.

[a] Abbreviations: FSD, female sexual dysfunction; FSAD, female sexual arousal disorder; VIP, vasoactive intestinal peptide; NEP, neutral endopeptidase; ACE, angiotensin converting enzyme; ECE, endothelin converting enzyzme; WSCDI, ((1-[3-(dimethylamino)propyl]-3-ethylcarbodiimde); EEDQ, (2-ethoxy-1-ethoxycarbonyl-1,2-dihydroquinoline); Lawesson's reagent, (2,4-bis(4-methoxyphenyl)-1,3-dithia-2,4-diphosphetane-2,4-disulfide); Burgess' reagent, (methoxycarbonylsulfamoyl-triethylammonium hydroxide); HOBt, 1-hydroxybenzotriazole.

10.1021/jm060133g CCC: $33.50
Published on Web 06/15/2006

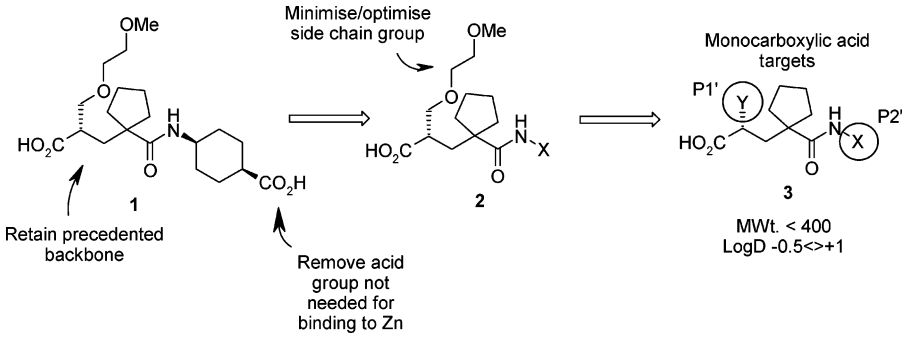

Figure 1. Evolution of the strategy of targeting small monocarboxylic acid NEP inhibitors, starting from Candoxatrilat **1** and optimizing the amide substituent X and the P_1' substituent Y.

Table 1. Elimination Half-life and Selected Properties of Short $T_{1/2}$ Carboxylic Acid Drugs[9]

drug	$T_{1/2}$ (h)	MWt.	cLogP	TPSA (Å^2)
Amoxicillin	1	365	0.6	158
Baclofen	3.8	214	1.6	63
Ciprofloxacin	3.7	331	1.3	75
Diclofenac	1.5	318	3.3	49
Flurbiprofen	5.5	244	4.1	37
Fluvastatin	0.7	411	3.6	83
Furosemide	1.4	331	2.9	131
Gabapentin	6.5	171	1.2	63
Ibuprofen	2	206	3.7	37
Ketoprofen	1.8	254	2.8	54
Sulindac	7	356	3.6	74
Tolmetin	7	257	1.6	59

relationships of a range of these selective monocarboxylic acid NEP inhibitors are described below.

Targeting Acids as *prn* Agents. There are many carboxylic acids, some of them zwitterions, exemplified in the clinic covering a wide range of elimination half-lives.[9] The majority of them tend toward short $T_{1/2}$, such as aspirin (salicyclic acid), the penicillin-type antibiotics, and the quinolone-type antibiotics (see Table 1). In targeting a *prn* treatment for FSAD, short $T_{1/2}$ is precisely what is required. An analysis of the marketed acids with $T_{1/2}$ <8 h indicated that most were of small size (MWt. <365) and/or of relatively low LogP (<3). The topological polar surface area (TPSA) cutoff for these orally absorbed compounds was around 140 Å^2, consistent with prior experience at Pfizer and allowing for a slightly higher value of the actively absorbed amoxicillin.[10] These agents are either excreted unchanged in the urine (i.e., producing no circulating metabolites) or where metabolism is seen, it is dominated by glucuronidation of the acid function and CYP2C9-mediated oxidative metabolism. There were very few examples where a marketed acid has both a high molecular weight (>400) and is lipophilic (LogP > 3).

Many of the acids in Table 1 also display very high levels of binding to serum albumin (>99%) and high unbound clearance, especially the more lipophilic examples, leading to higher efficacious dose requirements, a situation that is not conducive with an ideal, low dose *prn* profile; indeed, some COX inhibitors require the daily dosing of hundreds of milligrams up to more than 1 g.

Our analysis of these data was that we should aim to produce the majority of our target structures with a molecular weight under 400 and relatively high polarity (LogD <1). The very polar penicillins make use of active transport mechanisms for oral absorption,[10] which we would not be able to guarantee for our agents, and therefore, we decided to aim for around −0.5 to 0 LogD as the bottom end of the ideal lipophilicity range. The likelihood was that our acids would probably also be quite highly bound to serum albumin and possibly even very highly bound. We, therefore, chose to target quite high potency (hNEP IC_{50} of <50 nM).

Enzyme Structure. NEP (EC.3.4.24.11) is a 750 amino acid zinc-dependent enzyme first isolated in the 1970s. It is a Type II membrane protein with a short *N*-terminal cytoplasmic domain followed by a 23-residue hydrophobic domain and a large extracellular domain containing the active site.[11] It has a relatively broad substrate specificity and is capable of cleaving a variety of substrates in both the CNS and periphery, with cleavage preferentially occurring on the amino side of hydrophobic residues, such as Phe, Met, and Leu,[12] which suggests the presence of a lipophilic S_1' binding region. This is reflected in many of the potent NEP inhibitors reported in the literature possessing a hydrophobic group adjacent to the Zn-binding function. The Roche group has recently reported the crystal structure of one such nonselective inhibitor, phosphoramidon (**4**) co-crystallized with human recombinant NEP.[13] At the outset of our work, however, no such detailed knowledge of the NEP structure was available, and all of the structural data in the literature was based on the related bacterial enzyme thermolysin (TLN).

Thermolysin is a readily crystallized, thermostable 316 residue enzyme that has a relatively poor primary sequence homology with NEP but shares many of the same substrates, is inactivated by the same inhibitors as NEP, and has the same stereochemical dependence.[14] Structural analogies have been drawn between the active sites of TLN and NEP, and through the work of Roques and others,[14,15] homology models based on TLN crystallographic data and computational overlap of sequence data have been used to design potent NEP inhibitors. The 3D structure of the combined ACE/NEP inhibitor thiorphan **5** bound to thermolysin was reported in 1989, and the key contacts are depicted below.[16]

The lipophilic benzyl group projects into a large and hydrophobic S_1' subsite, whereas the central amide bond is involved in a network of H bonds to the enzyme, and the sulfur atom binds the zinc ion as its thiolate anion. Interestingly, a crystallographic comparison of thiorphan and the reversed amide retrothiorphan **6** bound to thermolysin showed that the amide N and O atoms maintained essentially equivalent H-bond interactions with the Asp and Arg residues of the enzyme, and indeed, both of these agents share excellent NEP potency. Further, a glutaramide inhibitor that contains much of the functionality of our targets has been shown to make many of the same contacts with thermolysin as does thiorphan.[17] Acidic groups in the S_2' region bind to a key Arg residue, and it is this interaction that our target monoacids would be lacking. The *C*-terminal region of TLN shows very low homology with NEP and represents a relatively undefined area of the enzyme. As

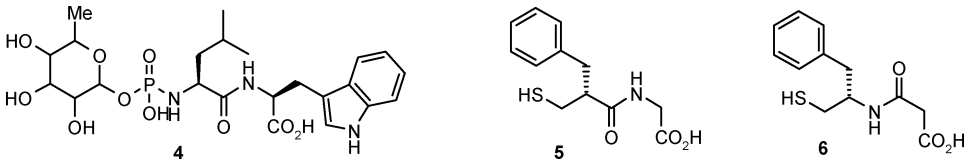

Figure 2. Structures of ACE/NEP inhibitors phosphoramidon **4**, thiorphan **5**, and retrothiorphan **6** for which crystal structures in either a NEP construct or bacterial thermolysin are reported.

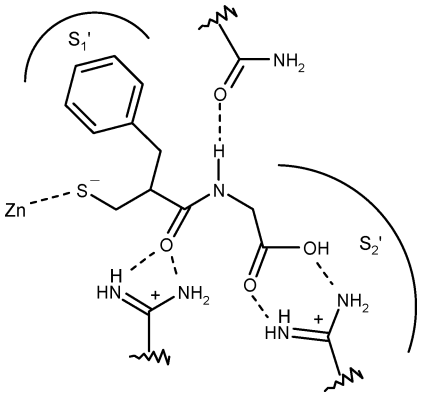

Figure 3. Drawing of the key contacts that thiorphan makes with the S_1' and S_2' regions of bacterial thermolysin.

such, we were uncertain at the outset of this work as to the levels of both potency and selectivity we could expect from a monoacid series and the manner in which neutral amide substituents would bind to the S_2' region of NEP.[18] We, therefore, saw diversity as being crucial in our initial SAR investigations, with subsequent targets being directed according to emerging trends in NEP activity.

Synthetic Chemistry. A protected form of the glutaric acid template is easily constructed by the alkylation of cyclopentane carboxylic acid dianion (Scheme 1).[19,20] The initial SAR was generated with an *n*-propyl substituent adjacent to the Zn-binding acid. This was best constructed in a 2-step allylation−reduction sequence. The coupling of commercially available amines to this acid was then performed using WSCDI ((1-[3-(dimethylamino)propyl]-3-ethylcarbodiimde) with *N*-methylmorpholine (NMM) as the base. For reactive amines (e.g., primary alkylamines), dichloromethane (DCM) at room temperature was sufficient to achieve complete reaction. For less active amines (e.g., amino-substituted heterocycles), dimethylformamide (DMF) or acetonitrile (MeCN) at elevated temperatures were required for good yields of the coupled products, although the 3-ethyl pyridine (**16**) was consistently formed in very poor yield. The ester protecting group could then be removed using standard protocols to deliver the requisite acids in excellent yields. This chemistry was sufficiently robust and reliable to allow many of the coupling reactions to be performed in parallel on a milligram scale in a 96-well plate format. The reactions were monitored by TLC, the evaporation of volatiles was carried out in a Genevac vacuum centrifuge, and the crude residues were purified by automated HPLC using ELSD-MS to detect products. The contents of those wells containing product were combined, evaporated, and diluted robotically and then sent for biological assaying.

The indane methanol compound **21** is known,[20] and the synthesis of both the indane methanol unit and **21** itself are described therein. Noncommercial amines were prepared by the procedures described in Schemes 2−11 and then coupled to acid **7** in a fashion identical to that described in Scheme 1.

Thus, a 1-ethyl-1,2,3-triazole was synthesized by simple alkylation of 4-nitro triazole[21] with ethyl iodide using sodium

Scheme 1[a]

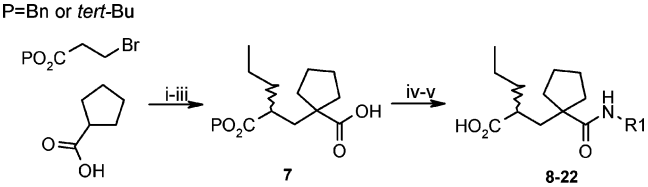

[a] Reagents and conditions: (i) 2 equiv LDA, THF, −78 °C → room temperature, 16 h, 90%; (ii) 2 equiv LDA, allyl bromide, THF, −78 °C → room temperature, 16 h, 92%; (iii) 15 psi H_2, EtOH, 10% Pd/C, room temperature, 91%, (iv) R1NH_2, WSCDI, HOBt. NMM, solvent (see text), 25−100 °C, 16 h, 60−99%; (v) For P═Bn, 30 psi H_2, 10% Pd/C, room temperature, 5−16 h; for P = ^{t}Bu, TFA/DCM (1:1), room temperature, 6−16 h or HCl (g), Et_2O, room temperature, 15 min, 15−98%.

Table 2. *n*-Pr-*spiro*-cyclopentyl Glutaramides Synthesized According to Scheme 1

Compound	R^1	Compound	R^1	Compound	R^1
8		**13**		**18**	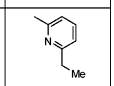
9		**14**		**19**	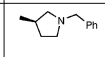
10		**15**		**20**	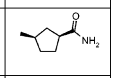
11		**16**		**21**	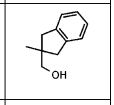
12		**17**		**22**	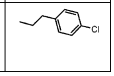

hydride as the base (Scheme 2). The choice of DMF was found to be critical to produce a homogeneous mixture and a complete reaction. This reaction led to an appreciable amount of the isomeric 3-ethyl analogue, which was easily separable by silica gel chromatography. Hydrogenation of the separated **24** under Pd/C catalysis then formed amino triazole **25** in quantitative yield.

4-Amino-pyrimidine (**27**) was prepared starting from the commercially available 2-amino-4-hydroxy pyrimidine. Chlorination with $POCl_3$ gave the corresponding chloroamine, which was then aminated with propylamine to provide **27** in modest yield.

The 4-methoxypyrazine target **29** in Scheme 4 was prepared by sequential methoxylation and amination of 3,6-dichloropyrimidine, both steps proceeding in excellent yield.

A short series of pyridyl targets were synthesized according to Schemes 5−7. First, 2-amino-4-benzyl pyridine was prepared in three steps from 2,4-dibromopyridine (Scheme 5). Selective monolithiation at the 4-position with ^{n}BuLi in ether, followed by quenching with benzaldehyde gave benzylic alcohol **31**, which was aminated with aqueous ammonia in the presence of copper (II) sulfate in a sealed vessel. Deoxygenation was then carried out by hydrogenation with catalytic palladized charcoal

Scheme 2[a]

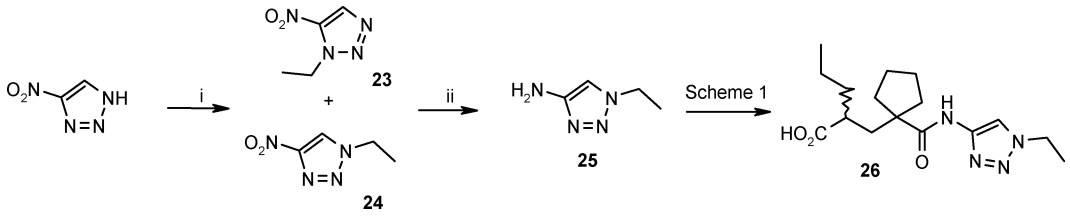

[a] Reagents and conditions: (i) NaH, DMF, 0 °C, 3 h, then silica gel chromatography, 57% (1-isomer), 21% (3-isomer). For the 1-isomer: (ii) 15 psi H_2, Pd/C (10%), EtOH, 4 h, 100%.

Scheme 3[a]

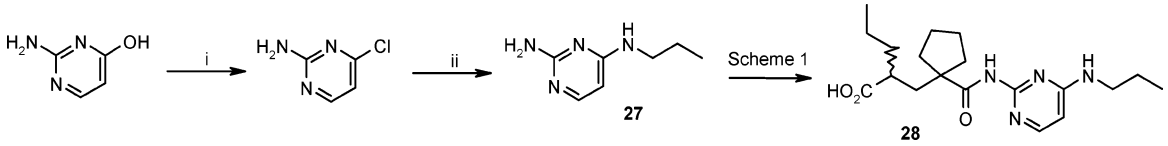

[a] Reagents and conditions: (i) $POCl_3$, 100 °C, 4 h, 52%; (ii) ^{n}PrNH$_2$, ^{i}Pr$_2$EtN, DMF, 90 °C, 16 h, 26%.

Scheme 4[a]

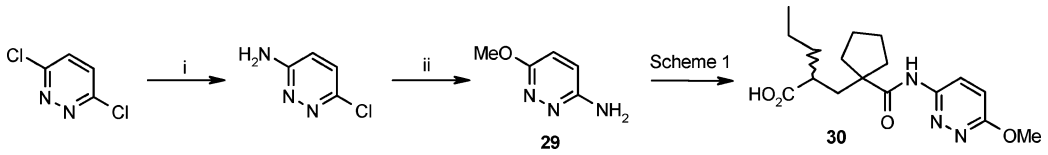

[a] Reagents and conditions: (i) 0.88 NH_3, DCM, 35 °C, 6 h, 91%; (ii) NaOMe, MeOH, steel bomb, 140 °C, 4 h, 94%.

Scheme 5[a]

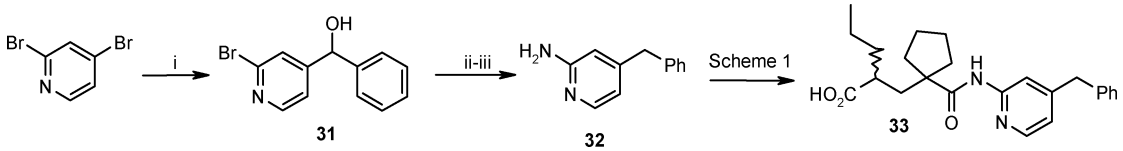

[a] Reagents and conditions: (i) ^{n}BuLi, Et_2O, −78 °C then PhCHO, −78 °C → room temperature, 16 h, 68%; (ii) 0.88 NH_3, Cu(II)SO_4·5H_2O, sealed tube, 135 °C, 24 h, 83%; (iii) 30psi H_2, Pd/C (5%), 1 M HCl, EtOH, room temperature, 6 h, 78%.

Scheme 6[a]

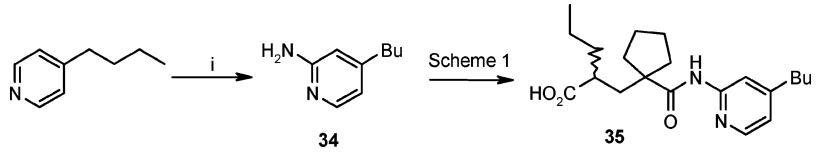

[a] Reagents and conditions: (i) $NaNH_2$, xylene, 150 °C, 16 h, 38%.

Scheme 7[a]

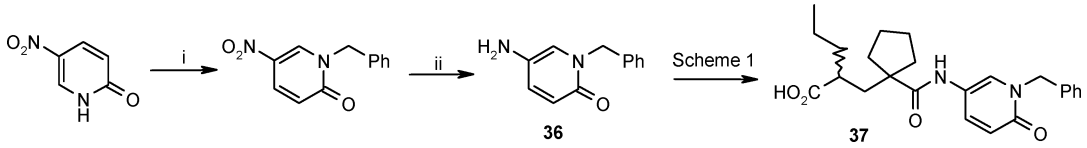

[a] Reagents and conditions: (i) NaH, LiBr, BnBr, DME/DMF, 70 °C, 16 h; (ii) Sn, cHCl, 90 °C, 1.5 h, 51%.

(5%) in acidic ethanol as solvent and the resulting amine **32** coupled to **7** as before.

Commercially available 4-butyl pyridine was simply heated at 150 °C in xylene with sodamide overnight using a slight modification of the literature method.[22] Chichibabin conversion provided the requisite aminopyridine **34** in modest yield.

The benzyl-pyridone of Scheme 7 was made from 5-nitro-2-pyridone, the sodium anion of which was simply alkylated with benzyl bromide in the presence of lithium bromide in a mixture of dimethoxyethane (DME) and DMF.[23] These conditions were reported to improve the proportion of N-alkylation relative to O-alkylation, and in our hands, none of the corresponding *O*-benzyl analogue was detected. Mild reduction with metallic tin in hydrochloric acid provided the 5-amino analogue **36**, which was then coupled to **7** as before.

Several 5-substituted 1,3,4-thiadiazoles were prepared by reaction of the appropriate acid chloride with thiosemicarbazide,[24] followed by warming for several hours, until all evolution of gas had ceased. Prolonged reaction times or higher reaction temperatures led to a significantly reduced yield of 2-amino-

Scheme 8[a]

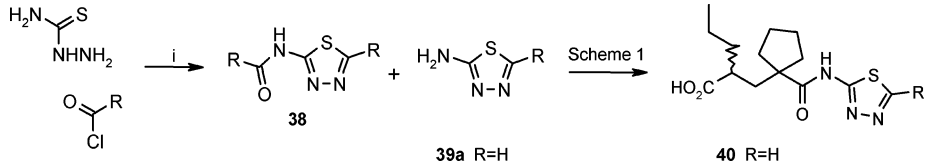

39a R=H
39b R=Ph
39c R=iBu
39d R=Bn
39e R=cyclopropylmethyl

40 R=H
41 R=Ph
42 R=iBu
43 R=Bn
44 R=cyclopropylmethyl

[a] Reagents and conditions: (i) Thiosemicarbazide, (no solvent), 40 °C, 4 h, then separation by flash chromatography, 28−53%.

Scheme 9[a]

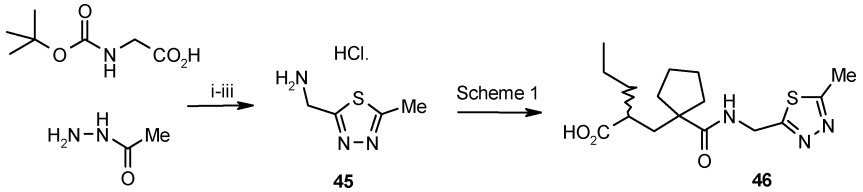

[a] Reagents and conditions: (i) EEDQ, DCM, room temperature, 16 h, 37%; (ii) Lawesson's reagent, THF, room temperature-70 °C, 3 h then room temperature, 16 h, 89%; (iii) HCl (g), DCM, 0 °C, 15 min then N_2, room temperature, 1 h, 100%.

Scheme 10[a]

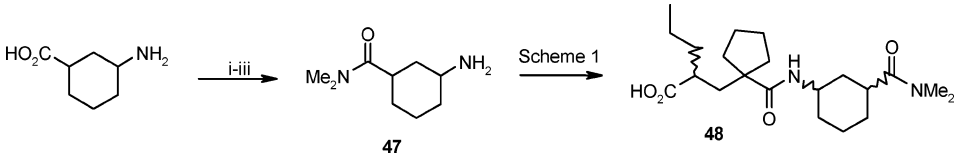

[a] Reagents and conditions: (i) BOC_2O, NaOH, dioxan, 0 °C → room temperature, 16 h, 81%; (ii) Me_2NH, WSCDI, HOBt, NMM, DMF, room temperature, 16 h, 66%; (iii) TFA, DCM (1:1 v/v), room temperature, 4 h, 55%.

Scheme 11[a]

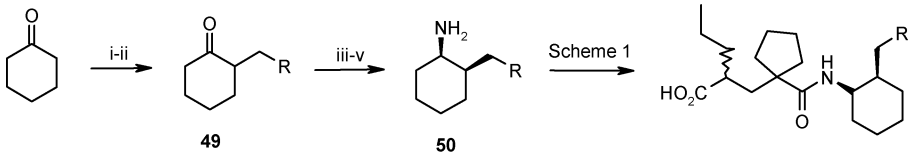

51 R=Ph
52 R=Et

[a] Reagents and conditions: (i) LDA, allyl bromide, THF, −78 °C → room temperature, 16 h, 23% (**49**, R═Ph commercially available); (ii) 30 psi H_2, Pd/C (10%), EtOH, room temperature, 16 h, 52%; (iii) *R*-(+)-1-Phenyl-ethylamine, *p*-TsOH, toluene, reflux, 24 h, 100%; (iv) 120 psi H_2, RaNi, EtOH, room temperature, 48 h, 7−15%; (v) 120 psi H_2, Pd/C (10%), EtOH, 45 °C, 16 h, 89−94%.

thiadiazole products **39** and appreciable amounts of 2-amido-thiadiazoles **38**, where the requisite amine appears to form first and then reacts with excess acid chloride in situ (Scheme 8).

A related 2-aminomethyl-1,3,4-thiadiazole (**45**) was synthesized in excellent yield by the initial coupling of *N*-BOC glycine with acylhydrazide using EEDQ (2-ethoxy-1-ethoxycarbonyl-1,2-dihydroquinoline) as the coupling agent. Cyclodehydration aided by Lawesson's reagent (2,4-bis(4-methoxyphenyl)-1,3-dithia-2,4-diphosphetane-2,4-disulfide) formed the thiadiazole ring, and simple treatment with gaseous hydrogen chloride revealed the amine, which was coupled to **7** as above.

Several cyclohexylamines were synthesized in one of three ways. A 1,3-disubstituted aminocyclohexylamide (**47**) was prepared from the corresponding amino-cyclohexane carboxylic acid by an N-carbamoylation, amidation, and N-deprotection sequence. The final product was obtained as a mixture of all possible diastereoisomers.

In contrast, two 1,2-disubstituted amino-cyclohexylamines were formed using enolate chemistry to introduce the alkyl substituent onto the cyclohexane ring **49**.[25] The *cis*-1,2 arrangement was secured by the hydrogenation of a nonracemic phenethylimine, which occurs specifically from the face opposite that occupied by the adjacent alkyl substituent to furnish the racemic cis diastereomer **50** in low yield.[26] This was then coupled to the glutarate template as before, and the esters deprotected to furnish the final acids.

Finally, the 1,4-disubstituted analogue of the aminocyclohexylamine described in Scheme 10 was best prepared by first installing cyclohexane ring **53** onto substrate **7** and then appending the amide group afterward.

A phenethyl variation at the P_1' region was prepared in a manner entirely analogous to that described in Scheme 1. The dianion of glutarate **57**[19,20] was alkylated with phenethyl bromide in good yield and then coupled to 2-amino-5-ethyl-1,3,4-thiadiazole according to Scheme 1. Direct amide coupling of **57** yielded compound **60** (Y═H).

In the case of alkyl analogues of the *n*-propyl group, simple homologation of allyl acid **61**[19,20] was carried out by ozonolytic olefin cleavage, followed by Wittig condensation and hydrogenation of the ensuing double bond to provide acids **62**, which were then coupled to 2-amino-5-ethyl-1,3,4-thiadiazole.

A small series of oxadiazole amide bioisosteres were prepared from the corresponding carboxylic acid by the initial formation of bis acyl hydrazides **65**, followed by cyclodehydration

Scheme 12[a]

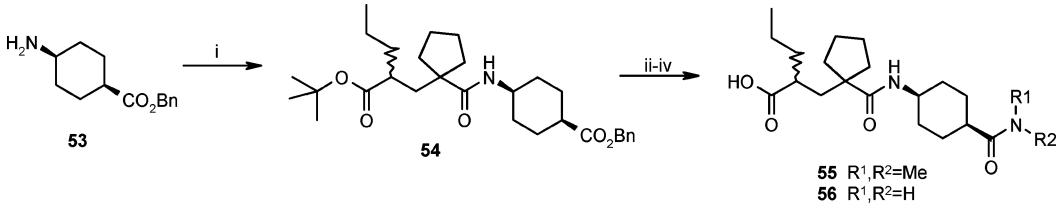

[a] Reagents and conditions: (i) See Scheme 1; (ii) 15 psi H_2, Pd/C (10%), room temperature, 16 h, 93%; (iii) R^1R^2NH, WSCDI, HOBt, NMM, DMF, room temperature, 16h, 58−71%; (iv) TFA, DCM (1:1 v/v), room temperature, 4 h, 65−91%.

Scheme 13[a]

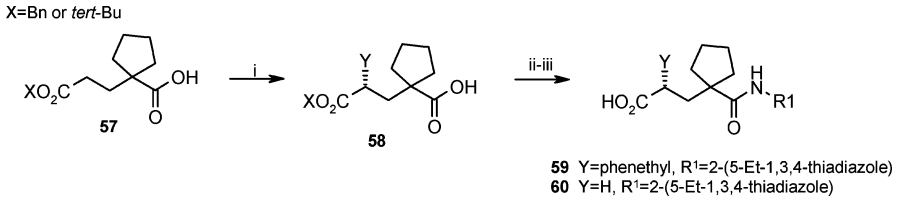

[a] Reagents and conditions: (i) 2 equiv LDA, THF, phenethyl bromide, −78 °C → room temperature, 16 h, 76%; (ii) WSCDI, 2-amino-5-ethyl-1,3,4-thiadiazole, HOBt, NMM, DMF, 25−100 °C, 16 h, 73−89%; (iii) See Scheme 1.

Scheme 14[a]

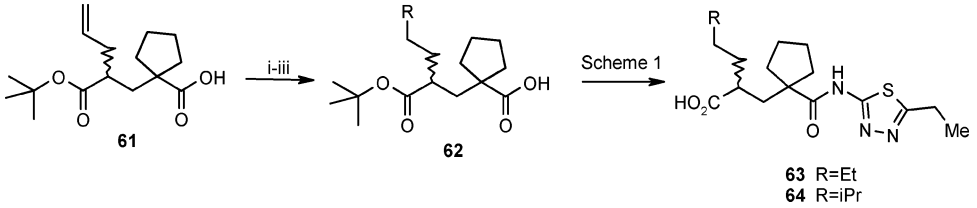

[a] Reagents and conditions: (i) O_3, DCM, −78 °C, 3 h, then DMS, room temperature, 3 h, 100%; (ii) 2 equiv Ph_3P═CHR, THF, 0 °C, 16 h, 17−20%; (iii) 15 psi H_2, Pd/C (10%), EtOH, room temperature, 6 h, 100%.

Scheme 15[a]

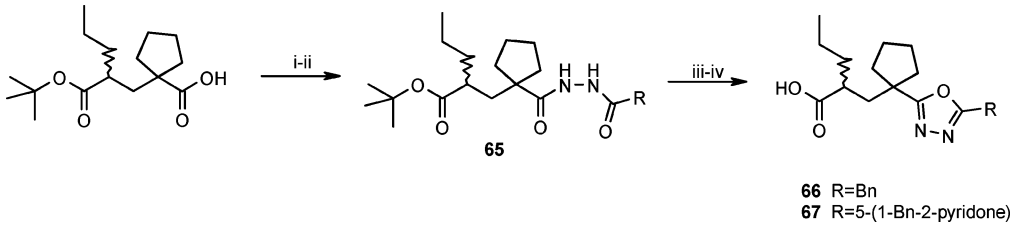

[a] Reagents and conditions: (i) CDI, HOBt, THF, hydrazine, 0 °C, 1 h, 100%; (ii) RCO_2H, WSCDI, HOBt, NEt_3, DCM, room temperature, 16 h, 67−92%; (iii) Burgess' Reagent, THF, reflux, 16 h, 82−89%; (iv) TFA, DCM (1:1 v/v), room temperature, 3 h, 69−84%.

Scheme 16[a]

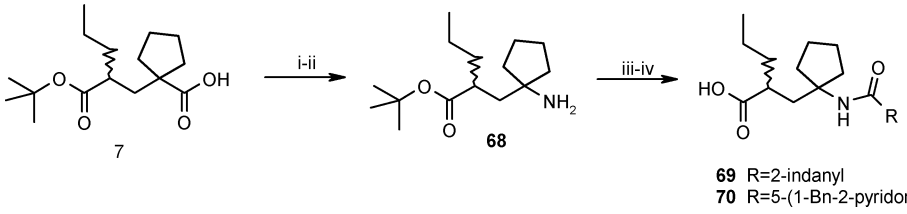

[a] Reagents and conditions: (i) $(PhO)_2P(O)N_3$, THF, reflux, then BnOH, 2.5 h, 80%; (ii) 15 psi H_2, Pd/C, EtOH, room temperature, 16h, 71%; (iii)) RCO_2H, WSCDI, HOBt, NEt_3, DCM, room temperature, 16 h, 26−59%; (iv) TFA, DCM (1:1 v/v), room temperature, 15 h, 63−99%.

promoted by Burgess' reagent (methoxycarbonylsulfamoyl-triethylammonium hydroxide).

Reversed amides were synthesized from ester **7** by a Curtius rearrangement of the derived acyl azide. The best yield was obtained when the ensuing isocyanate was quenched with benzyl alcohol, and the resulting benzyl carbamate then deprotected to amine **68** by hydrogenation. The coupling of acids to this amine then proceeded smoothly under the usual coupling conditions.

Tertiary *N*-methyl amides were prepared directly from the corresponding secondary amide by a simple deprotonation/methylation sequence (Scheme 17).

Results and Discussion

Compounds were first evaluated as inhibitors of canine NEP (dNEP) in vitro using a spectrophotometric assay, wherein the fluorescent product Abz-D-Arg-Arg is formed by the cleavage of *o*-aminobenzoyl-D-Arg-Arg-Leu-ethylenediamine-2,4-dini-

Scheme 17[a]

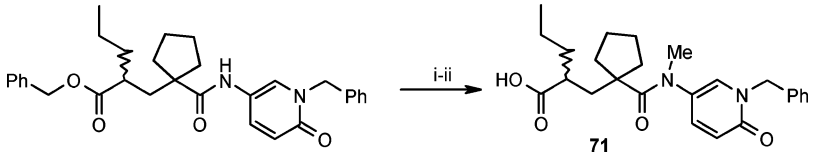

[a] Reagents and conditions: (i) NaH, MeI, THF, 0 °C, 6 h, 21%; (ii) 15 psi H_2, Pd/C, EtOH, room temperature, 16 h, 100%.

Table 3. Canine NEP Activity (IC_{50}) for Various Substituted Glutaric Acid Monoamides[a]

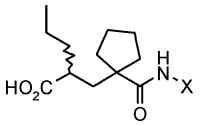

Compound	X	dNEP (nM)	Compound	X	dNEP (nM)
9	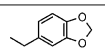	1500	**14**		384
10		176	**22**	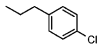	>2000
8		1710	**15**		>2000
11		530	**26**		82
21	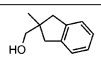	96	**28**	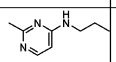	>2000
12		313	**30**		374
13		60			

[a] Mean data of at least two determinations. All entries are racemic mixtures. All compounds showed IC_{50} >3 μM activity vs dACE (data not shown) except for **15**, **22**, and **28**, which were not tested.

trophenyl.[27] Soluble NEP was obtained from the canine kidney cortex by an adaptation of a literature method.[28] Selectivity over canine ACE (dACE) and human ECE-1 (hECE-1) was established using *o*-aminobenzoyl-Gly-*p*-nitro-Phe-Pro-OH and big ET-1 as substrates, respectively. Potent and selective compounds were then assayed against human NEP (hNEP) and progressed into pharmacokinetic evaluation. The primary amino acid sequence of human NEP is >90% identical to that of other mammalian species, where the sequence is known. Sequence conservation is highest around the region that makes up the active site, and at the outset of this work, we did not predict any particular differences in activity of our series of glutaramides in dog vs human-derived NEP. Promising compounds that emerged from this analysis were assessed for efficacy in an animal model of genital blood flow.[34]

Initial Amide SAR. Many of the initial series of amides prepared were relatively weak inhibitors of NEP (Table 3). Flexible side chains, such as those in **9** and **22** showed the least activity against NEP (>1.5 μM). Removing some of this flexibility by alkyl substitution on the side chain improved the activity 3-fold (**11**, 530 nM). In a similar vein, the cyclopentylmethanol group in **8** was only weakly active (1710 nM), whereas when combining the hydroxymethyl function into a benzyl template, **14** showed modest activity (384 nM). Fusing a phenyl group onto the cyclopentane improved binding potency approximately 5-fold (**12**, 313 nM), and by combining the functionality in both **8** and **12**, a further 3-fold potency gain was made to give our first sub-100 nM inhibitor **21** (96 nM). Converting this amino-carbocycle into an amino-heterocycle gave mixed results. Although 1,3,4-thiadiazoles **10** and **13** showed good activity (176 and 60 nM, respectively), methyl pyridine **15** was only weakly active (630 nM). Similarly, although 1,2,3-triazole **26** demonstrated appreciable potency (82 nM), amino-pyrimidine **28** and methoxypyrazine **30** were much weaker. A possible explanation for this SAR could lie in the dipole moments of these heterocycles. Both thiadiazole and 1,2,3-triazole have significant dipoles toward the N atoms and could act as mimics of a carboxylate anion and thereby bind to the S_2' Arg suggested from the TLN modeling studies. This dipole would also be present to a large extent in a pyrazine ring, but the lower activity of **30** could be compromised by the methoxyl group clashing with a hydrophobic region of the enzyme.

Nonetheless, from this first wave of compounds, we were very encouraged to see some good potency in these small monoacids, and some general trends were apparent. A small carbo or heterocycle attached directly to the amide N atom provided several potent examples, provided there was no polar (H-bonding) group present on the ring. Rather, a lipophilic substituent (alkyl or phenyl) on such a small ring gave the most potent compounds of all. These SARs pointed strongly toward the amide S_2' substituent projecting into a hydrophobic region of the enzyme from an appropriately configured scaffold. Especially encouraging was the finding that the more active compounds from Table 3 were well within our ideal range of physical properties (e.g., **13**; $LogD^{25}$ 0.5, MWt 339). Equally encouraging was the finding that all compounds made showed exquisite selectivity over the related metallopeptidase ACE.

Pyridyl Amides. We reasoned that the Me group attached to the pyridine ring of **15** was possibly neither large enough nor suitably placed to provide optimal binding. This assertion was vindicated by the observation that unsubstituted pyridine **17** was a very weak inhibitor of NEP (>1 μM) and that both 6-ethyl pyridine **18** and 3-ethyl pyridine **16** were even less active. Further, extending the 4-Me group of **15** to either an ^{n}Bu (**35**, 184 nM) or a benzyl group (**33**, 96 nM) improved activity. Switching from a benzyl pyridine to an *N*-benzyl pyridone **37** lost NEP potency. It appeared that an appropriately situated lipophilic group on a pyridyl scaffold could offer good NEP activity in this series.

Thiadiazolyl Amides. A set of results very similar to that with the pyridyl series was seen with the 1,3,4-thiadiazole series. Unsubstituted heterocycle **40** was only weakly active against NEP (377 nM) and some 6-fold weaker than the ethyl case **13**. Both phenyl thiadiazole **41** and isobutyl analogue **42** were also weaker than **13** (some 4-fold and 2-fold, respectively). However, both benzyl expression **43** and cyclopropylmethyl compound **44** were found to be 2-fold more active than **13**, which again points to a specific lipophilic interaction between the heterocycle substituent and the enzyme. The 3-fold difference in activity between the isobutyl group of **42** and the cyclopropylmethyl of

44, and the 10-fold difference between the phenyl group of **41** and the benzyl group of **43** is testament to the specificity of this interaction. Inserting a CH_2 spacer between the amide N atom and the thiadiazole ring resulted in a large drop in activity, similar to the trends that were seen in Table 1.

The thiadiazole series again demonstrates that achieving good potency from a substituted, planar heterocyclic series is possible. There was a clear spatial preference for the substituent on these heterocycles such that small variations in the substituent or its conformation produced quite substantial changes in activity. It was unclear whether these features would translate to a nonplanar carbocyclic series.

Carbocyclic Amides. To allow an examination of areas of the S_2' binding site as yet unexplored in the heterocyclic series, several saturated five and six-membered ring amide groups were prepared with a range of substitution, conformational preference, and polarity. We reasoned that the alkyl substituents appended to the thiadiazole and pyridyl rings were being directed by the ring scaffold away from the trajectory of the amide bond and that this trajectory was key to good potency. A carbocyclic ring would offer a much more flexible scaffold from which to append groups at various positions around the ring. The first couple of targets looked at both a small alkyl and a benzyl group anchored in a cis conformation to the amine on a cyclohexyl template. Benzyl compound **51** was some 4-fold more active than its propyl counterpart **52** but still some 6-fold less potent than benzyl thiadiazole **43**. Inherent in moving to a cyclohexyl template is an increase in LogP of this substituent, and having observed no significant breakthroughs with the first couple of lipophilic examples from the cyclohexyl series, all further targets featured more polar substituents. The first of these were dimethyl amides in a 1,4 and a 1,3 arrangement (**55** and **48**, respectively), which were both around 300 nM inhibitors. Moving to some much more polar amide groups, pyrrolidine **19** showed only micromolar potency, whereas surprisingly, a primary amide appended to both a cyclopentyl **20** and a cyclohexyl **56** ring proved to be the most active examples in the series at 213 and 150 nM, respectively. These cis fused ring systems were severalfold more potent than their trans analogues (data not shown) and seemed to refute some of the observed intolerance of polar substituents suggested in Table 3. However, even the most active example from this series was still 3-fold less potent than some of the heterocyclic compounds above.

P_1' SAR. From the above data, several low MWt. potent NEP inhibitors had emerged. All of these compounds were racemic adjacent to the carboxyl group, and all incorporated an *n*-propyl group at this location. It was this area where our attention was now focused. Our choice of *n*-propyl had been driven largely by its small size and precedented NEP activity within a glutaramide template. From the thermolysin literature,[14] larger and more lipophilic groups projecting into the S_1' subsite would be expected to provide potency gains. Taking the 5-ethyl-1,3,4-thiadiazole as a representative example of an active S_2' amide substituent, several analogues of the *n*-propyl group were examined.

Extending the propyl group to butyl gives an essentially equipotent compound **63** (84 nM), and a further branching Me group in **64** loses a small amount of activity. Phenethyl analogue **59** did not produce any large potency gains, and removing the P_1' side chain lost only 4-fold binding potency. It was gratifying to discover that our SAR with an *n*-propyl substituent represented the most active P_1' group from within this limited SAR set of targets, and this knowledge, the ease of synthesis of the propyl chain, and its small size encouraged us to retain this as our favored group in the P_1' position.

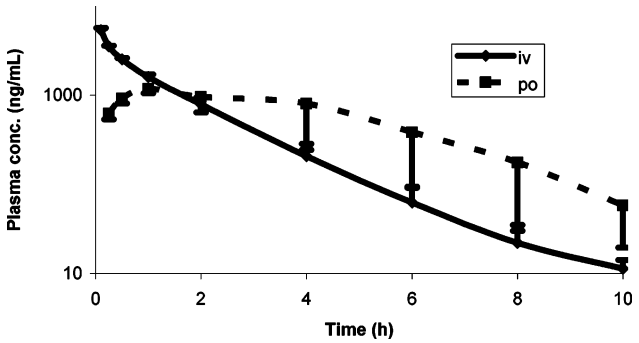

Figure 4. Plasma concentration time curve in male rats after iv or po administration of *R*-**13** (1 mg/kg).

Secondary Amide Isosteres. The final region of our series that was explored was the amide linkage. The literature structural information presented above suggested that a strong H-bond network to both the amide O atom and the NH group was important to activity. This was borne out by methylating the N atom of pyridone **37** to essentially destroy all activity in tertiary amide **71**. Similarly, the oxadiazole isosteres, which lacked an H-bond donating group, were only very weak inhibitors. Given the maintenance of NEP activity that was seen by switching from thiorphan to retrothiorphan, two reversed amides were synthesized (**69** and **70**), but this change lost almost all binding affinity. This latter result simply confirmed that thiorphan forms a different H-bond network to NEP and that SAR trends within the thiorphan series would be very difficult to track over to the current series of glutaramides. No further examples of amide-variant compounds were pursued.

Enantiomerically Pure Material. The NEP literature clearly establishes a stereochemical preference for substituents adjacent to the Zn-binding moiety.[14] In the case of the glutaramide-based Candoxatrilat, this preference is *R*, which we fully expected to be mirrored in our series of monoacids. This was confirmed by resolution of several members of the series, profiling the resolved enantiomers and confirming the absolute configuration of the eutomer by small molecule X-ray crystallography of the derivatives (data not shown).

The most promising compounds possessing good binding affinity, low MWt., and LogD[29] within our target range were identified as both methyl and ethyl thiadiazoles **10** and **13**, and indane methanol **21**. These compounds covered a LogD range of between 0.1 and 1.1 with molecular weights in the range 325−373. These were resolved by chiral HPLC and the individual enantiomers profiled.

Consistent with the Candoxatrilat series, the *R* enantiomers were found to be considerably more active than the *S*. All compounds were found to be exquisitely selective over hECE-1 and dACE, and the Caco-2 flux values were largely consistent with a combination of MWt. and LogD. The favorable balance of potency and physicochemistry led to *R*-**13** being chosen for further profiling in vitro and in vivo. Inhibitory IC_{50} values were obtained with *R*-**13** against several species of NEP, which were to be used to assess either pharmacokinetic (rat) or efficacy (rabbit) parameters, and were largely seen to agree well with the canine NEP inhibition values, within an approximately 2-fold window.

The pharmacokinetics of *R*-**13** were evaluated in the male and female rat (Figure 4 and Table 11). *R*-**13** exhibited a low clearance and a low volume of distribution resulting in a short elimination half-life of ca. 2 h. A clear sex difference was not

Table 4. Canine NEP Activity (IC_{50}) for Various Pyridyl Amides[a]

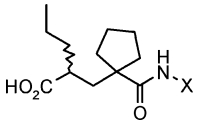

Compound	X	dNEP (nM)	Compound	X	dNEP (nM)
18		>2000	**35**	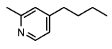	184
17		1500	**33**	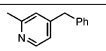	96
16		1710	**37**	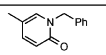	313

[a] Mean data of at least two determinations. All entries are racemic mixtures. All compounds showed IC_{50} >3 μM activity vs dACE (data not shown) except for **16** and **18**, which were not tested.

Table 5. Canine NEP Activity (IC_{50}) for Various Thiadiazolyl Amides[a]

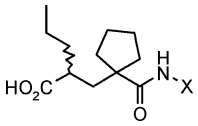

Compound	X	dNEP (nM)	Compound	X	dNEP (nM)
40		377	**43**	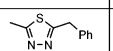	30
41		283	**44**	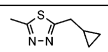	38
42		124	**46**	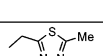	700

[a] Mean data of at least two determinations. All entries are racemic mixtures. All compounds showed IC_{50} >3 μM activity vs dACE.

Table 6. Canine NEP Activity (IC_{50}) for Various Cyclohexyl Amides[a]

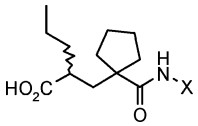

Compound	X	dNEP (nM)	Compound	X	dNEP (nM)
51		195	**19**	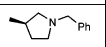	1060
52		890	**20**	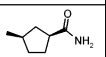	213
55	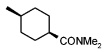	370	**56**	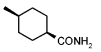	150
48	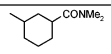	297			

[a] Mean data of at least two determinations. All entries are racemic mixtures. All compounds showed IC_{50} >3μM activity vs dACE.

evident, although female rats showed a trend toward higher systemic clearance and higher volume (Table 11).

The PK parameters given in Table 11 do not reflect the complete picture of the potentially sex specific disposition of *R*-**13** in the rat; female rats exhibited a renal clearance significantly higher than that of males (0.86 vs 0.03 mL/min/kg). Similar sex differences in the renal excretion of carboxylic acids have been observed before[30] and could be due to a sex specific expression of the transport protein oatp1a1 (aka oatp1; gene symbol *slco1a1*, formerly *slc21a1*) in the apical tubular membrane.[31] The insignificant PK sex difference in the rat can possibly be attributed to the predominant elimination of *R*-**13** via UGT enzymes, where major sex differences in expression are not yet completely understood.[32] The exact UGT enzymology in the rat was not further investigated. There was no difference in the quantity and quality of circulating oxidative metabolites in male and female rats (data not shown). Consequently, the oxidative metabolism of *R*-**13** in the rat was shown to be mainly due to the sex unspecific cyp2c6 with minor contributions from cyp3a1 and cyp1a1 (Figure 5).

The male specific cyp3a2, cyp2c11, cyp2c13, and the female specific cyp2c12[33] did not metabolize *R*-**13**.

Given that the medicinal chemistry strategy for this program was based on the maintenance of low molecular weight and LogD, it was interesting to compare the above pharmacokinetic profile with that of a larger and more lipophilic compound. *R*-**13** had a PK profile superior to that of *R*-**21** (Table 12). In line with its higher lipophilicity, *R*-**21** showed 4−5 times higher unbound clearance than *R*-**13**. The pharmacokinetics of enantiomerically pure *R*-**21** were not significantly different from that of the racemate *rac*-**21** (Table 12 and Figure 6) suggesting that both enantiomers undergo similar pharmacokinetic processes.

Efficacy. The combination of unbound clearance and potency favored the progression of *R*-**13** into the rabbit model of sexual arousal.[4b,34] In this model, the rabbit pelvic nerve is stimulated

Table 7. Canine NEP Activity (IC_{50}) for Various P_1' Analogues[a]

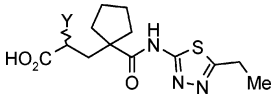

Compound Number	Y	dNEP (nM)
63		84
60	H	237
59		46
64		120

[a] Mean data of at least two determinations. All entries are racemic mixtures. All compounds showed IC_{50} >3 μM activity vs dACE.

Table 8. Canine NEP Activity (IC_{50}) for Various Amide Isosteres[a]

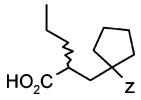

Compound	Z	dNEP (nM)	Compound	Z	dNEP (nM)
71	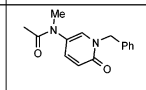	>10000	**70**	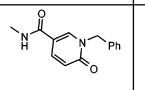	>3000
67	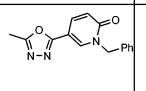	1139	**69**	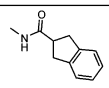	>3000
66	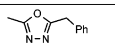	3100			

[a] Mean data of at least two determinations. All entries are racemic mixtures. All compounds showed IC_{50} >3 μM activity vs dACE except for **69**, **70**, and **71**, which were not tested.

Table 9. NEP Inhibitory Activity (IC_{50}) and Physicochemical Data for Enantiomerically Pure Versions of **10**, **13**, and **21**[a]

racemate compd	MWt	LogD	TPSA (Å^2)	*R*-enant. potency, dNEP (nM)	*S*-enant. potency, dNEP (nM)	*R*-enant. Caco-2 P_{app}, AB/BA ($\times 10^{-6}$ cm s^{-1})	*R*-enant. HLM (min)	*R*-enant. RLM (min)
10	325	0.1	120	114	286	<1/2	>120	nd[b]
13	339	0.5	120	26	292	9/14	>120	>120
21	373	1.1	87	11	205	6/10	62	>120

[a] Mean data of at least two determinations. All compounds showed IC_{50} >3 μM activity vs dACE and hECE-1, except for *S*-**10**, which was not tested against ECE-1. All compounds showed <10% inhibition against a wide panel of receptors, ion channels, and enzymes when tested at 10 μM. Caco-2 flux was measured at pH7.4/7.4 and 25 μM. LogD was measured in 1-octanol/water at pH 7.4. Metabolic stability (substrate disappearance) was determined in human liver microsomes at 1 μM substrate and 0.5 μM CYP. [b] nd not determined.

Table 10. Inhibitory NEP Potency of *R*-**13** against Several Species of NEP[a]

compd	hNEP IC_{50} (nM)	dNEP IC_{50} (nM)	ratNEP IC_{50} (nM)	rabbitNEP IC_{50} (nM)	recombinant hNEP IC_{50} (nM)
R-**13**	18.9	23.7	14.3	10.2	19.7

[a] Mean data of at least two determinations.

to simulate the neuronal effects of sexual arousal, and changes to both the vaginal and clitoral blood flow are monitored using laser doppler sonography. The effects of intravenously administered compounds can be assessed directly over extended periods of time. The performance of *R*-**13** in this model has been published elsewhere.[34c] It is important to note that there is no effect on the basal (i.e., unstimulated) blood flow or on any cardiovascular parameters. The onset of the effect on vaginal blood flow is noticeable after the first administration of compound, in keeping with its pharmacokinetic profile. Translating these direct blood flow measurements into a dose−response curve provides an EC_{50} value for *R*-**13** of approximately 36 nM free drug, which shows a 33% potentiation of vaginal blood flow.[34c] The rabbit IC_{50} value for *R*-**13** was measured at 10.2 nM, which is in good agreement with the measured EC_{50} value. The maximal response was seen at approximately 10 × IC_{50}, that is, 100 nM free drug with the response starting to peak at potentially lower concentrations than this one. *R*-**13** thus demonstrates excellent efficacy in this rabbit model of sexual arousal and was expected to be similarly efficacious in humans. This compound was, therefore, chosen for clinical evaluation as a potential treatment for FSAD.

Conclusion

We have shown that relatively small (MWt. <400) 2-aminopyridines and 2-amino-1,3,4-thiadiazoles with hydrophobic substituents at the 4- and 5-positions, respectively, are potent and selective inhibitors of NEP. Incorporating various substitution patterns at the P_1' position is tolerated, and changes in this region, in conjunction with those at the S_2' hydrophobic binding region allows a range of compounds to be prepared with disparate LogD. Pharmacokinetic profiling in animals has suggested that a profile that is suited to *prn* dosing in humans

Table 11. Rat Pharmacokinetic Parameters for *R*-**13** at 1 mg/kg (iv and po)[a]

sex	CL (mL/min/kg)	V_d (L/kg)	$T_{1/2}$ (h)	T_{max} (h)	C_{max} (ng/mL)	f_u	*F* (oral) (%)
males	3.0 ± 0.3	0.4 ± 0.1	1.7 ± 0.3	1	1176 ± 124	0.106 ± 0.009	103 ± 46
females	4.7 ± 1.2	0.9 ± 0.4	2.1 ± 0.7	1	1462 ± 120	0.13 ± 0.026	131 ± 58

[a] Mean data ± standard deviation of three animals. Jugular vein cannulated rats were dosed at 1 mg/kg iv (tail vein) and po (gavage). The blood samples were withdrawn via the indwelling catheter until 24 h post-dose. Results for CL, V_d, and $T_{1/2}$ were compared with Student's *t*-test and found to be not significantly different (p >0.05).

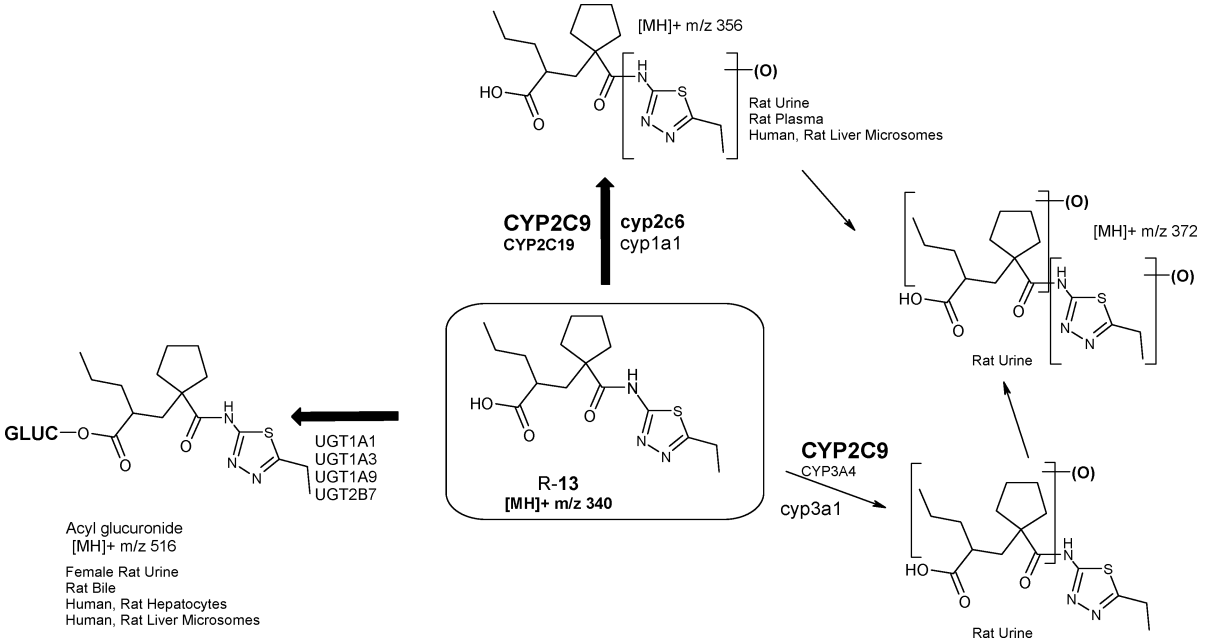

Figure 5. Metabolic pathways of *R*-**13**. Human enzymes are written in upper case and rat enzymes in lower case letters.

Table 12. Rat Pharmacokinetic Parameters for **21** at 1 mg/kg (iv and po)[a]

compd	CL (mL/min/kg)	V_d (L/kg)	$T_{1/2}$ (h)	T_{max} (h)	C_{max} (ng/mL)	f_u	F (oral) (%)
R-**21**	34.8 ± 4.0	4.7 ± 1.8	1.5 ± 0.5	0.25	233 ± 177	0.243 ± 0.036	144 ± 11
rac-**21**	22.6 ± 9.8	3.9 ± 2.1	2.0 ± 0.2	0.25	311 ± 130	nd	108 ± 42

[a] Mean data ± standard deviation of three animals. Jugular vein cannulated rats were dosed at 1 mg/kg iv (tail vein) and po (gavage). The blood samples were withdrawn via the indwelling catheter until 24 h post-dose; nd: not determined. The results for CL, V_d, and $T_{1/2}$ were compared with Student's *t*-test and found to be not significantly different ($p > 0.05$).

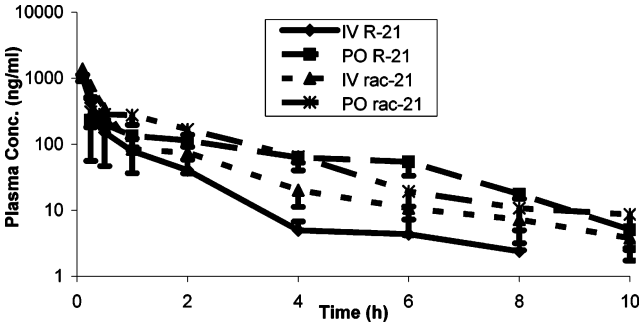

Figure 6. Plasma concentration time curve in male rats after iv or po administration of *R*-**21** or *rac*-**21**(1 mg/kg).

is achievable with this class of compound, from which *R*-**13** was chosen for further clinical evaluation.

Experimental Section

General. Melting points were determined on a Gallenkamp Melting point apparatus using glass capillary tubes and are uncorrected. Unless otherwise indicated, all reactions were carried out under a nitrogen atmosphere, using commercially available anhydrous solvents. Thin-layer chromatography was performed on glass-backed precoated Merck silica gel (60 F254) plates, and flash column chromatography was carried out using 40−63 μm silica gel. Proton NMR spectra were measured on a Varian Inova 300 or 400 spectrometer in the solvents specified. Mass spectra were recorded on a Fisons Trio 1000 using thermospray positive (TSP) ionization. Combustion analyses were conducted by Exeter Analytical U.K., Ltd., Uxbridge, Middlesex. Where analyses are indicated only by the symbols of the elements, the results obtained are within 0.4% of the theoretical values. The purity of compounds was carefully assessed using analytical TLC and proton NMR, and the latter technique was used to calculate the amount of solvent in solvated samples. The pK_a measurements were performed by Sirius Analytical Instruments Ltd., Forest Row, East Sussex. In multistep sequences, the purity and structure of intermediates were verified spectroscopically by ^{1}H NMR. Optical rotations were determined using a Perkin-Elmer 341 polarimeter. Optical purity was determined by an analytical HPLC analysis of preparative HPLC-resolved material (see below) via a comparison to the racemic material.

1-(2-*tert*-Butoxycarbonyl-ethyl)-cyclopentanecarboxylic Acid (57). A 2.5 M solution of ^{n}BuLi in hexanes (42 mL, 105 mmol) was added dropwise to a stirred solution of diisopropylamine (15 mL, 107 mmol) in 100 mL of THF at −20 °C under nitrogen and the whole solution was stirred at this temperature for 30 min. A solution of cyclopentane carboxylic acid (5.7 g, 50 mmol) in 10 mL of dry THF was then added dropwise and the resulting solution stirred at −20 °C for 30 min, and then at room temperature for 2 h. The solution was then re-cooled to −20 °C and *tert*-butyl bromopropionate (11 g, 53 mmol) was added portionwise and the mixture then stirred at room temperature for approximately 2 h. Then, 150 mL of diethyl ether and 110 mL of 2 N HCl solution were added in sequence, and the organic layer was separated, dried over $MgSO_4$, and evaporated to a yellow oil. This oil was taken up in diethyl ether (100 mL) and washed with saturated $NaHCO_3$ until almost all of the starting cyclopentane carboxylic acid was no longer present by TLC. The organics were then washed with 2 N HCl solution, separated, dried, and evaporated in vacuo to provide 4.5 g of a yellow oil, which slowly solidified on standing. This solid was recrystallized from approximately 15 mL of hexane to provide 1.49 g of the title compound as a white solid.

1-(2-*tert*-Butoxycarbonyl-pent-4-enyl)-cyclopentanecarboxylic Acid (61). A 2.5 M solution of ^{n}BuLi in hexanes (3.5 mL, 105 mmol) was added dropwise to a stirred solution of diisopropylamine (15 mL, 107 mmol) in 100 mL of THF at −20 °C under nitrogen, and the whole solution was stirred at this temperature for 30 min. The solution was cooled to −65 °C and, a solution of **57** (970 mg, 4 mmol) in 5 mL THF was added dropwise over approximately 10 min. And the whole solution was then stirred at this temperature for 40 min. Allyl bromide (0.4 mL, 4.6 mmol) was added in one portion, and the reaction was allowed to warm up to room temperature slowly over 6 h. Then, 50 mL of diethyl ether was added, followed by 9 mL of 2 N HCl solution, and the organic layer was separated, dried over $MgSO_4$, and evaporated in vacuo to give a yellow oil. This oil was purified by column chromatography using 30%, then 50% diethyl ether in pentane as an eluant to provide the title compound as a clear oil (1.05 g).

1-(2-*tert*-Butoxycarbonyl-pentyl)-cyclopentanecarboxylic Acid (7). Compound **61** (900 mg, 3.2 mmol) was taken up in 15 mL of EtOH and hydrogenated at 30 psi hydrogen pressure in the presence of 10% palladized charcoal (90 mg) in a bomb for 6 h. The suspension was filtered through a short plug of Arbocel, and the filtrate was evaporated to dryness in vacuo to provide the title compound as a clear oil (900 mg). In the case where a benzyl in place of a *tert*-Bu protecting group was used, an identical procedure was used in each of the above three steps starting with benzyl bromopropionate, providing the benzyl ester as a clear oil.

General Procedure 1: Amide Formation. The requisite amine derivative (1 equiv) and acid **7** (1 equiv) were dissolved in DMF, DCM, or MeCN (1 M) and NMM added in one portion. HOBt (1 equiv) was then added, followed by 1 equiv of WSCDI. The mixture was typically heated at 100 °C for 12 h under a nitrogen atmosphere or until reaction was complete as judged by TLC analysis. After cooling to room temperature, the mixture was diluted with EtOAc and washed several times with water. The organic layer was separated, washed with water, dried ($MgSO_4$), and evaporated to afford the desired amides, which were purified by flash chromatography using mixtures of either pentane and EtOAc or MeOH and DCM, depending on the polarity of the individual products.

General Procedure 2: Amide Formation in Parallel. The requisite amine derivatives (30 μmoles) were weighed into the wells of a solid Al 96-well block and 1 equiv of DMF solutions of the reagents described in procedure 1 introduced into each well by a Eppendorf micropipet. 1.1 equiv of a DMF solution of **7** was also added to each well and the block agitated overnight while heating to ca. 100 °C. After cooling to room temperature, 2 mL of water was added to each well and the contents filtered through a hydrophobic frit. Then, 1 mL of TFA was added to the filtrates and the block once again agitated overnight at room temperature. Volatiles were removed in a Genevac vacuum centrifuge, and the residues purified by automated HPLC (Gilson 305 pumps, Gilson 215 injection/fraction collection, and Polymer Laboratories PL-ELS1000 ELSD detection).

General Procedure 3: *tert*-Butyl Ester Deprotection. The requisite *tert*-butyl ester (1 equiv) was dissolved in a 1:1 mixture of TFA and DCM (0.25 M total) and the reaction mixture stirred at room temperature under a nitrogen atmosphere overnight. The reaction mixture was evaporated and then partitioned between DCM and water. The organic layer was separated, washed several times

with water, dried ($MgSO_4$), then evaporated, and the residue purified by flash chromatography on silica gel to afford the desired acid. Alternatively, the *tert*-butyl ester was dissolved in either Et_2O, DCM, or EtOAc and HCl gas bubbled through the solution at room temperature for 10 min. The solution was then purged by bubbling through N_2 gas for a further 10 min and then evaporated to dryness. The residue was purified by flash chromatography on silica gel to afford the desired acids.

General Procedure 4: Benzyl Ester/Carbamate Deprotection. The requisite benzyl ester was dissolved in EtOH or MeOH (0.4M) in a stainless steel bomb and a catalytic quantity of palladized charcoal (either 5 or 10% concentration, 1−5% w/w with substrate) added cautiously. H_2 pressure was then applied to the vessel (between 15 and 30 psi) and the contents magnetically stirred overnight. The catalyst was filtered through a short plug of arbocel (2 cm) and the filtrate evaporated to dryness under reduced pressure. The residue was then purified by flash chromatography on silica gel.

General Procedure 5: 2-Amino-1,3,4-thiadiazole Ring Formation. The requisite acid chloride (2 equiv) (obtained either commercially or by treatment of the acid with $(COCl)_2$ in DCM) was heated with thiosemicarbazide (1 equiv) in the absence of solvent at 40 °C for 4 h. During this time, all evolution of gas ceased, and water was added. The crude reaction mixture was basified to pH 12 with a 50% aqueous solution of NaOH. The solution was then concentrated in vacuo and azeotroped several times, first with toluene and then EtOAc to remove traces of water. The residue was then purified by silica gel chromatography using 3%, 5%, and then 10% MeOH in DCM as the eluant to provide the amino-thiadiazole as a white solid (typically 80−90% yield) along with small quantities of the N-acylated material. Provided the temperature is maintained below 40 °C and reaction times below 6 h, the formation of this side-product is largely avoided.

General Procedure 6: *cis*-1,2-Disubstituted Cyclohexane Formation. Cyclohexanone (1 equiv) was added to a stirred solution of lithium diisopropylamide (1 equiv) in dry THF (0.4 M total concentration) at −78 °C under nitrogen and the mixture stirred at this temperature for 45 min. A solution of the electrophile (1 equiv) in dry THF was added dropwise over 30 min, and stirring was continued for a further 30 min before the reaction was allowed to slowly warm up to room-temperature overnight. The bright orange reaction mixture was cooled to 0 °C and quenched with 2 N HCl. The solvent was removed in vacuo and the mixture extracted with EtOAc. The combined extracts were washed with brine, dried ($MgSO_4$), and evaporated to an orange oil, which was purified by flash chromatography (SiO_2; Et_2O in pentane). The purified oil was taken up in toluene and *R*-1-phenyl-ethylamine (1 equiv) added in one portion. *p*-TsOH (cat.) was added in one portion and the whole solution refluxed overnight in a flask fitted with a Dean and Stark apparatus. The solvent was then evaporated to a white solid, which was taken up in EtOH and RaNi (cat.) added in one portion and the mixture hydrogenated at 4 bar H_2 pressure and room temperature for 2 days. A further portion of RaNi was added, and hydrogenation continued for a further 2 days. Water was added and the crude mixture filtered through a short plug of Arbocel, and the solid was washed with water and EtOH. Evaporation provided an oil, which was purified by flash chromatography (SiO_2; MeOH (5%) in DCM) to yield a clear oil, which was dissolved in EtOH, and HCl gas was bubbled through the solution for 30min. The mixture was evaporated to low volume and then flooded with ether to precipitate a white solid, which was collected by filtration. This solid was dissolved in EtOH and hydrogenated at 4 bar H_2 pressure with 10% Pd/C (cat.) as the catalyst at 45 °C overnight. Filtration through a short plug of Arbocel and evaporation of the filtrate provided a white solid of the *cis*-2-alkyl-1-amino-cyclohexylamine, which could be coupled to **7** with no further purification.

General Procedure 7: Installing the P_1' Substituent (Alkylation of 57). Glutarate **57**[19,20] (1 equiv) was added to a stirred solution of lithium diisopropylamide (2.2 equiv) in dry THF (0.27 M total concentration) at −78 °C under nitrogen and the mixture stirred at this temperature for 45 min. A solution of the electrophile (1.1 equiv) in dry THF was added dropwise over 30 min, and stirring was continued for a further 30min before the reaction was allowed to slowly warm up to room temperature overnight. The bright orange reaction mixture was cooled to 0 °C and quenched with 2 N HCl. The solvent was removed in vacuo and the mixture extracted with EtOAc. The combined extracts were washed with brine, dried ($MgSO_4$) and evaporated to an orange oil, which was purified by flash chromatography (SiO_2; EtOAc in pentane). The products were isolated as pale yellow oils. Characterization data are given in ref 20.

General Procedure 8: Installing the P_1' Substituent (Homologation of 61). Ozone (excess) was bubbled through a stirred solution of allyl acid **61**[20] (1 equiv) in DCM at −50 °C for 30 min. After this time, a persistent blue color developed, and oxygen gas was then bubbled through the solution for 5 min before DMS (5 equiv) was added in one portion. The resulting colorless solution was allowed to warm up slowly to room temperature overnight under a nitrogen atmosphere and then evaporated to dryness. The residue was redissolved in DCM, washed with water, dried ($MgSO_4$), and evaporated to afford a colorless oil of the aldehyde, which was used without any further purification. To a stirred solution of the phosphonium salt (2 equiv) in dry THF at 0 °C under N_2 was added a solution of ^{n}BuLi (2.5 M solution in hexanes, 2 equiv) and the resulting suspension stirred for 30 min. To the resulting orange solution was added dropwise a solution of the aldehyde from the previous step (1 equiv) in dry THF, and the whole solution was stirred at room temperature for 4 h. The solvent was evaporated, and the residue partitioned between DCM and 2 N HCl. The organic layer was separated, dried ($MgSO_4$), and evaporated to a solid, which was purified by flash column chromatography (SiO_2; EtOAc in pentane) to afford the desired olefin; R = CHMe. This olefin (1 equiv) was dissolved in EtOH and hydrogenated at 30 psi H_2 pressure overnight at room temperature with a catalytic amount of 10% Pd/C. The reaction mixture was filtered through a short plug of Arbocel, and the plug was then washed with EtOAc (×2) and concentrated in vacuo to afford the requisite alkane as a colorless oil, which was found to be sufficiently pure to be used with no further purification.

General Procedure 9: Oxadiazole Formation. The acid chloride derived from **7** was taken up in DCM and triethylamine (2 equiv) and hydrazine hydrate (1 equiv) added in one portion. After 3 h of stirring at room temperature, the reaction was quenched with water, the organic layer separated, dried, and evaporated to a yellow oil of the acyl hydrazide. The acyl hydrazide was taken up in DCM, triethylamine (1.5 equiv), and HOBt (1.02 equiv), and WSCDI (1.3 equiv) and the acid (1 equiv) added in one portion. The mixture was stirred at room temperature for 16 h and then washed with water and brine, dried ($MgSO_4$), and evaporated to a gum, which was purified by flash column chromatography (SiO_2; EtOAc in pentane) to give the bisacyl hydrazide. This was taken up in THF and 1.5 equiv of Burgess' reagent added in one portion, and the whole solution refluxed for 16 h. The reaction mixture was partitioned between 2% $NaHCO_3$ solution and EtOAc, and the organic layer was washed with water and brine, and then dried ($MgSO_4$) and evaporated to provide the oxadiazole analogue.

General Procedure 10: Preparation of Inverted Amides From (7). The acid **7**[20] (1 equiv) was taken up in dioxan (0.4 M) under nitrogen and triethylamine (2 equiv) and DPPA (1 equiv) added dropwise. The solution was heated at reflux for 2.5 h before benzyl alcohol (1.5 equiv) was added, and the reflux continued overnight. After cooling to room temperature, the mixture was quenched with 1 N NaOH and extracted with EtOAc (×3), dried ($MgSO_4$), and evaporated to give a crude oil, which was purified by flash chromatography (SiO_2; EtOAc (10%) in pentane) to give the benzyl carbamate. This was deprotected according to general procedure 4. The resulting amine was then coupled to the requisite acid according to general procedure 1.

4-Amino-1-ethyl-1,2,3-triazole (25). Step 1: 24. 4-Nitro-1,2,3-triazole (96 mg, 0.84 mmol) was dissolved in dry DMF (4 mL) at 0 °C under a nitrogen atmosphere before the portionwise addition of a 60% suspension of NaH in mineral oil (35 mg, 0.88 mmol)

over 10 min, followed by excess ethyl iodide. The reaction was allowed to reach room temperature and stirred for a further 3 h and then quenched by the addition of water (3 mL). The quenched mixture was extracted with EtOAc (2 × 30 mL), and the combined organic fractions were dried ($MgSO_4$) and evaporated to an oily residue. This residue was purified by silica gel chromatography (SiO_2; EtOAc (20%) in pentane), to provide the desired 1-ethyl isomer (284 mg, 57%) and the 3-isomer (106 mg, 21%), both as clear oils.

Step 2: 25. The product from step 1 (100 mg, 0.70 mmol) was dissolved in EtOH (8 mL) and placed in a stainless steel hydrogenation vessel. Then, 10 mg of 10% palladized charcoal was added carefully to the solution, and the vessel was then pressurized to 15 psi with hydrogen gas. The vessel was warmed to ca. 40 °C, the contents stirred for 4 h, and then allowed to cool to room temperature and vented. The reaction mixture was filtered through a 2 cm plug of arbocel, and the filtrate evaporated to a clear oil. This oil was purified by flash chromatography (SiO_2; MeOH (5%) in DCM) to afford the desired amino triazole as a clear oil (92 mg, 98%).

2-Amino-4-propylamino-pyrimidine (27). Step 1. 2-Amino-4-chloro-pyrimidine. 2-Amino-4-hydroxy-pyrimidine (10 g, 80 mmol) and $POCl_3$ (15 mL, 160 mmol) were refluxed together for 1.5 h. The reaction mixture was poured onto ice and then basified to pH 9 by the addition of solid Na_2CO_3. The solution was extracted with EtOAc (2 × 400 mL) and DCM (300 mL). The combined organics were dried over anhydrous $MgSO_4$, filtered, and evaporated to give an off-white solid, which was purified by flash chromatography (SiO_2; EtOAc (40 → 100%) in pentane) to give a white solid of the chloropyrimidine (5.9 g, 52%).

Step 2: 27. The product from step 1 (900 mg, 6.3 mmol) was heated at 90 °C with ^{n}Pr amine (655 μL), Hunigs base (2.2 mL, 12.6 mmol), and DMF (10 mL) under N_2 for 16 h. The cooled reaction mixture was diluted with EtOAc (20 mL) and then washed with water (4 × 10 mL). The organic layer was dried ($MgSO_4$), filtered, and evaporated to give an orange oil, which was purified by flash column chromatography (SiO_2; EtOAc (50%) in pentane, then MeOH (5%) in DCM) to a colorless solid (245 mg, 26%) of the amine.

3-Amino-6-methoxy-pyrazine (29). Step 1: 3-Amino-6-chloro-pyrazine. 3,6-Dichloropyrazine (500 mg, 3.36 mmol) was taken up in a mixture of DCM (4 mL) and NH_4OH solution (2 mL) and warmed at 35 °C for 6 h. The mixture was evaporated to dryness in vacuo and used in the next step without further purification.

Step 2: 29. The product from step 1 was taken up in MeOH (10 mL) and NaOMe (5 eq) added in one portion, and the whole solution was heated at 140 °C in a stainless steel bomb for 4 h. The reaction mixture was evaporated to dryness in vacuo and then purified by column chromatography using 2% MeOH in DCM as the eluant to give the product as an off-white solid. Yield 94%.

2-Amino-4-benzyl-pyridine (32). Step 1: 31. ^{n}BuLi (17 mL, 2.5 M in hexanes, 43 mmol) was added dropwise to a cooled (−78 °C) solution of 3,5-dibromopyridine (10 g, 42 mmol) in ether (200 mL) to maintain an internal temperature of < −70 °C. The mixture was stirred for 15 min before a solution of benzaldehyde (4.5 g, 43 mmol) in 20 mL of ether was added dropwise and the mixture stirred for 15 min before the cooling bath was removed and the contents allowed to warm to room temperature over 1 h. The reaction was quenched by the addition of an aqueous NH_4Cl solution (200 mL) and the organics extracted with ether, dried, and evaporated. The residual yellow oil was purified by flash chromatography (SiO_2; MeOH (5 → 20%) in DCM) to give the alcohol as a pale yellow oil (7.6 g, 68%).

Step 2. The product from step 1 (2 g, 7.6 mmol) and $CuSO_4 \cdot 5H_2O$ (350 mg, 1.4 mmol) in 0.88 NH_3 (18 mL) was heated at 135 °C in a sealed tube for 24 h. A NaOH solution (1 M, 10 mL) was added to the cooled solution and the mixture extracted with ether (6 × 20 mL). The combined extracts were dried ($MgSO_4$) and evaporated to low volume. The resulting precipitate was filtered, washed with ether, and dried to give the aminopyridine (1.3 g, 83%) as a white solid; mp 92−94 °C.

Step 3: 32. The product from step 2 (700 mg, 3.5 mmol) and 5% Pd/C (70 mg) in 1 M HCl (5 mL) and EtOH (20 mL) were hydrogenated (30 psi H_2, room temperature) for 6 h. The mixture was filtered through a 2 cm plug of Arbocel and the filtrate concentrated in vacuo and basified using aqueous $NaHCO_3$ solution. The organics were then extracted with DCM (3 × 50 mL), dried ($MgSO_4$), and evaporated under reduced pressure. The crude product was purified by flash chromatography (SiO_2; MeOH (8%) in DCM containing 0.4% NH_3 solution) to give the amine as a solid (500 mg, 78%); mp 107−109 °C.

2-Amino-4-butyl pyridine (34). A mixture of 4-butyl pyridine (5 g, 37 mmol) and 95% $NaNH_2$ (1.7 g, 41 mmol) in xylene (10 mL) was heated at 150 °C for 18 h. The cooled mixture was diluted with ether (100 mL) and extracted with 2 N HCl (×2). The extracts were basified with NaOH and re-extracted with ether. The combined extracts were dried ($MgSO_4$) and evaporated under reduced pressure to an oil, which was purified by flash chromatography (SiO_2; MeOH (3%) in DCM containing 0.15% NH_3 solution) to a white solid (2.1 g, 38%).

5-Amino-1-benzyl-2(1*H*)-pyridone (36). A mixture of 1-benzyl-5-nitro-1*H*-pyridin-2-one (1 g, 4.4 mmol) and granulated Sn (3.5 g, 30 mmol) were taken up in cHCl (14 mL) and heated at 90 °C for 1.5 h. The cooled solution was diluted with water (25 mL), neutralized with a Na_2CO_3 solution, and extracted with EtOAc (250 mL). The extract was dried ($MgSO_4$) and evaporated to give the aminopyridone as a pale green solid (440 mg, 51%).

2-Aminomethyl-5-methyl-1,3,4-thiadiazole Hydrochloride (45). Step 1. *N*-BOC glycine (5 g, 28.5 mmol) was dissolved in DCM (75 mL) at room temperature. EEDQ (7.96 g, 28.5 mmol) was added in one portion, followed by acetic hydrazide (2.6 g, 34.2 mmol) and the solution left to stir overnight at room temperature. The resulting solid was filtered off and dried under high vacuum to provide 2.42 g (37%) of the bisacyl hydrazide as white crystals.

Step 2: 45. The hydrazide from step 1 (500 mg, 2.16 mmol) was dissolved in dry THF (40 mL) at room temperature and Lawesson's reagent (960 mg, 2.4 mmol) added in one portion. The resulting suspension was then heated to reflux for 3 h and then allowed to cool to room temperature over 16 h. The volatiles were evaporated at reduced pressure and the resulting clear oil purified by flash chromatography (SiO_2; EtOAc (70%) in pentane) to provide the thiadiazole as a clear oil (483 mg, 91%), which crystallized on standing. This was further purified by dissolving in 100 mL of EtOAc and adding approximately 2 g of decolorizing charcoal. After stirring for 10 min, the mixture was filtered under a slight vacuum and the solvent evaporated to provide pure product (441 mg) as a white crystalline solid. This was taken up in DCM at 0 °C, and a slow stream of HCl gas bubbled through the solution via a micropipet for 15 min. The HCl stream was turned off and replaced with a slow stream of N_2 gas to purge most of the HCl from the solution. After 1 h of N_2 bubbling, the solvent was evaporated in vacuo to provide a white solid of the amine hydrochloride salt in a quantitative yield.

3-Amino-cyclohexane Carboxylic Acid Dimethyl Amide (47). 3-Amino-1-cyclohexane carboxylic acid (1 g, 6.9 mmol) was added to a mixture of 7 mL of 1 N NaOH solution in 7 mL of dioxan. The mixture was then cooled to 0 °C and di-*tert*-butyl-dicarbonate (1.67 g, 7.68 mmol) was added in one portion, followed by a slow warming up to room temperature overnight. The mixture was evaporated to a low volume (approximately 5 mL) in vacuo, and the aqueous solution was acidified with 2 N HCl solution to pH 1 and extracted with EtOAc (3 × 10 mL), and the extracts were combined, dried ($MgSO_4$), and concentrated in vacuo to afford a white solid (1.43 g). This solid was combined with dimethylamine (1.5 mL, 33% solution in absolute ethanol, 5.6 mmol), WSCDI (1.19 g, 6.2 mmol), HOBt (0.84 g, 6.2 mmol), and NMM (1.11 mL, 10.1 mmol) in DMF (30 mL) and stirred at room temperature for 16 h. The mixture was then evaporated to dryness in vacuo and chromatographed directly on silica gel using 5% MeOH in DCM as the eluant to provide 997 mg of a clear oil. This oil was dissolved in DCM (8 mL) and TFA (8 mL) and the whole solution was stirred at room temperature for 4h. The reaction mixture was

concentrated in vacuo, DCM (20 mL) was added, and the solution was washed with water (2 × 25 mL) and a saturated solution of $NaHCO_3$ (25 mL). The aqueous washes were combined, concentrated in vacuo to provide a white solid, which was purified by chromatography using 84:14:2 DCM/MeOH/NH_3 as the eluant to provide **47** as a colorless oil (346 mg).

2-[1-(5-Ethyl-[1,3,4]thiadiazol-2-ylcarbamoyl)-cyclopentylmethyl]-4-phenyl-butyric Acid (59). This compound was prepared in a fashion identical to that used to prepare compound **61** but using phenethyl bromide in place of allyl bromide to give intermediate **58**, which was then processed according to Scheme 1 to give the title compound as a clear oil.

3-[1-(5-Ethyl-[1,3,4]thiadiazol-2-ylcarbamoyl)-cyclopentyl]-propionic Acid (60). This compound was prepared directly from **57** according to Scheme 1 to give the title compound as a clear oil.

2-[(1-{[(1-Benzyl-6-oxo-1,6-dihydro-3-pyridinyl)−(methyl)-amino]-carbonyl}-cyclopentyl)-methyl]-pentanoic Acid (71). The benzyl ester of (**37**) (120 mg, 0.24 mmol) was dissolved in dry THF (3 mL) and cooled to 0 °C under nitrogen. A suspension of NaH (19 mg, 0.48 mmol, 60% suspension in oil) was added in one portion and the mixture stirred for 1 h at 0 °C. Methyl iodide (1.1 equiv, 0.30 mmol) was added in one portion, and the reaction mixture was stirred at 0 °C for 30 min and then allowed to warm up to room temperature over 3 h. The solution was concentrated to low volume (ca. 1 mL) and treated with 4 mL of saturated aqueous $NaHCO_3$ solution. The organics were extracted with EtOAc (2 × 10 mL), dried ($MgSO_4$), and evaporated to give a gum. This was purified by flash column chromatography (SiO_2; EtOAc (35 → 70%) in pentane) to give the methyl amide as a clear oil (26 mg, 21%). This was then deprotected according to general procedure 4.

General Procedure 11: HPLC Resolutions. HPLC resolutions were performed with either a Chiralpak AD or OD column, 25 × 2 cm at ambient temperature and using mixtures of hexane, IPA, and TFA as the solvent (typically, 70% hexane, 30% IPA, and 0.1% TFA). The flow rate was typically 10 mL/min, and the runs lasted for 20 min, and detection was carried out at 220 nm. HPLC resolved material was typically of >98%ee and was obtained from the HPLC fractions by evaporation to low volume, azeotroping with several aliquots of toluene followed by slow crystallization from diisopropyl ether at −4 °C. Simple filtration and drying in vacuo provided the *R*-enantiomeric material in typically 40−45% yield from the racemate.

The racemic acid (**13**, 824 mg) was resolved by HPLC using an AD column (hexane/IPA/TFA (85:15:0.2), 10 mL/min) as eluant to give the *S* enantiomer (R_T 7.6 min) as a white powder (400 mg) in 99.5%ee; $[\alpha]_D$ +3.8° (*c* 0.1 in MeOH) and the *R* enantiomer (R_T 6.2min) as a white powder (386 mg) in 99.5%ee; $[\alpha]_D$ −9.0° (*c* 0.1 in MeOH).

The racemic acid (**10**, 620 mg) was resolved by HPLC using an AD column (hexane/IPA/TFA (85:15:0.1), 10 mL/min) as the eluant to give the *S* enantiomer (R_T 7.5 min) as a white powder (298 mg) in 94.5%ee and the *R* enantiomer (R_T 6.6min) as a white powder (261 mg) in 99.2%ee; $[\alpha]_D$ −11.9° (*c* 1.0 in MeOH).

The racemic acid (**21**, 204 mg) was resolved by HPLC using an OD column (hexane/IPA/TFA (95:5:0.1), 10 mL/min) as the eluant to give the *R* enantiomer (R_T 11.8 min) as a white powder (83 mg) in 99.5%ee; $[\alpha]_D$ −10.9° (c 0.46 in MeOH) and the *S* enantiomer (R_T 9.8 min) as a white powder (62 mg) in 99.5%ee; $[\alpha]_D$ +10.4° (c 0.67 in MeOH).

NEP Inhibition Assay. In a 96-well microtiter plate, 100 mL of fluorescent NEP substrate peptide (50 mM *o*-aminobenzoyl-D-Arg-Arg-Leu-ethylenediamine 2,4-dinitrophenyl) was added to 50 mL of 4 times the test concentration of inhibitor solutions. The assays were initiated by the addition of 50 mL of enzyme, which had been previously diluted such that with an incubation time of 1 h the percentage of substrate converted to product was approximately 10% or less. The reaction was incubated for 1 h at 37 °C in a shaking incubator and then stopped by the addition of 100 mL of 300 nM phosphoramidon. Samples corresponding to 100% substrate to product conversion were included to enable the percent substrate proteolyzed to be determined. Each assay point was in duplicate. Each IC_{50} experiment used a 10 point dilution series at half-logarithmical inhibitor concentration increments, with the highest concentration either 10, 1, or 0.1 mM. After the 1 h of incubation, the fluorescence of the samples was measured (Ex_{320}/Em_{420}) using a BMG Fluostar Galaxy reader and an IC_{50} value calculated using a customized Microsoft Excel add-in. The enzyme and substrate were prepared in 50 mM Tris·Cl, (pH 7.4 at 37 °C), and 4× inhibitor dilutions were made in 50 mM Tris·Cl at pH 7.4 at 37 °C/4% DMSO. Standard compounds assessed in this assay were as follows: phosphoramidon 0.71 nM, thiorphan 3.85 nM, and Candoxatrilat 2.61 nM.

Table 13. Variability of the Primary NEP Inhibition Assay

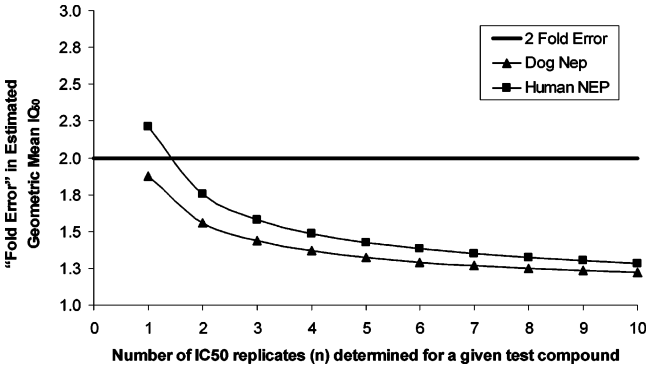

The IC_{50} estimates stated for NEP represent the geometric mean of at least 2 values obtained using separately weighed and solubilized compound samples. The NEP assay was highly reproducible. We demonstrated this from a statistical analysis of 25 IC_{50} values obtained from a single compound, which was tested multiple times over an 8 month period. By assessing the assay-to-assay variation, we were able to conclude that two replicates would be sufficient to ensure that the geometric mean IC_{50} was estimated with less than 2-fold error, on the basis of the width of the 95% confidence interval.

ACE Inhibition Assay. This assay was performed as described above for the NEP assay, except that the substrate used was *o*-aminobenzoyl-Gly-Gly-p-nitro-Phe-Pro-OH at a final assay concentration of 10 mM, and the enzyme and substrate buffer were 50 mM Tris·Cl at pH 7.4 (at 37 °C) and 300 mM NaCl, and the reaction was terminated using 100 mL of a 2 mM EDTA solution.

ECE-1 Inhibition Assay. Human recombinant ECE-1 was harvested from the growth media of Chinese Hamster Ovary (CHO) cells transiently transfected with an expression plasmid encoding the extracellular domain of ECE-1 (amino acids 73−753). ECE-1 was assayed in 100 mM HEPES-KOH at pH 7.0/1% DMSO using 1 μM big ET-1 peptide as the substrate. Following a 1 h incubation at 37 °C, the assay was terminated by the addition of an equal volume of 10 mM EDTA and the conversion of big ET-1 to ET-1 measured using an ELISA (Amersham Pharmacia RPN 228). The quantity of enzyme to use was determined as the dilution giving a final ELISA OD reading of approximately 1.0. Inhibitors were included in the assay at a range of concentrations, and their effects measured as % inhibition.

Pharmacokinetic Studies. Male CD rats (Charles River, Manston, UK) were used. These were jugular vein cannulated under general anaesthesia, with the cannula exteriorized at the back of the neck. At specified times after dosing, 0.2 mL samples of blood were withdrawn from the cannula and transferred to heparin tubes. Following adequate mixing, the blood samples were centrifuged, and plasma was generated. Immediately after that the plasma was stabilized by the addition of 0.01 parts of phosphoric acid (85%, v/v) and stored deep frozen until analysis. The fraction unbound in rat plasma was determined at 1 μg/mL using equilibrium dialysis against an isotonic Krebs−Ringer bicarbonate buffer (pH 7.4). The concentrations of glutaramides in rat plasma were determined by LC-MS-MS (Hewlett-Packard HP1100 binary HPLC pump, CTC

Pal Autosampler, Sciex API 2000 mass spectrometer with TurboIonSpray interface) at a flow rate of 1 mL/min, split 50:1 postcolumn using an Acurate flow splitter. Test compounds were extracted from 100 μL of acidified plasma mixed with 400 μL of 50 mM ammonium formate buffer (pH 3.5) using activated C18 IST cartridges in 96-well format (Porvair). The cartridges were washed with 1 mL of 50 mM ammonium formate (pH 3.5). The compounds were eluted with 1 mL of acetonitrile containing 5% (v/v) formic acid and evaporated to dryness under nitrogen at 20 °C. The residues were resuspended in 200 μL of 2 mM ammonium acetate in 70:30 (v/v) methanol/water (pH 3.5), and 180 μL was injected into the HPLC mass spectrometer. The mobile phase was 2 mM ammonium acetate in methanol/water (90/10; v/v; pH 3.5), and the column was a Hypersil HS100 C18, 5 μm, 50 $\times$ 4.6 mm. Detection was by positive ion multiple reaction monitoring (MRM) at Q1 and Q3 resolution of ca. 0.7 Da peak width at half-height (for *R*-**13**, Q1 340, Q3 130). The curtain gas, nebulizer gas, and TurboIonSpray gas were nitrogen at settings of 30 (CUR), 25 (GS1), and 40 (GS2), respectively. TurboIonSpray temperature was 100 °C. The collision gas was nitrogen at a setting of 2. The collision energy was 25 eV (OR 30 V), and the dwell time was 200 ms with 50 ms pause. All other data was obtained using standard methods.

Supporting Information Available: Full experimental details and characterization data. This material is available free of charge via the Internet at http://pubs.acs.org.

References

(1) Maw, G. N.; Stobie, A.; Planken, S.; Pryde, D. C.; Sanderson, V.; Platts, M. Y.; Corless, M.; Stacey, P.; Wayman, C.; Van Der Graaf, P.; Kohl, C.; Coggon, S.; Beaumont, K. The Discovery of Small Molecule Inhibitors of Neutral Endopeptidase: Structure-Activity Studies on Functionalised Glutaramide. *Chem. Biol. Drug Des*. **2006**, *1*, 74−77.

(2) Leiblum, S. R. Definition and Classification of Female Sexual Disorders. *Int. J. Impotence Res.* **1998**, *10*, S104−S106.

(3) (a) Frank, E.; Anderson, C.; Rubinstein, D. Frequency of Sexual Dysfunction in 'Normal' Couples. *N. Eng. J. Med.* **1978**, *299*, 111−115. (b) Rosen, R. C.; Taylor, J. F.; Leiblum, S. R.; Bachmann, G. A. Prevalence of Sexual Dysfunction in Women. *J. Sex Marital Ther.* **1993**, *19*, 171−188.

(4) (a) Goldstein, I.; Berman, J. R. Vasculogenic Female Sexual Dysfunction: Vaginal Engorgement and Clitoral Erectile Insufficiency Syndromes. *Int. J. Impotence Res.* **1998**, *10*, S84−S90. (b) Park, K.; Goldstein, I.; Andry, C.; Siroky, M. B.; Krane, R. J.; Azadzoi, K. M. Vasculogenic Female Sexual Dysfunction: The Haemodynamic Basis for Vaginal Engorgement and Clitoral Erectile Insufficiency. *Int. J. Impotence Res.* **1997**, *9*, 27−37.

(5) (a) Ottesen, B.; Gerstenberg, T.; Ulrichsen, H.; Manthorpe, T, Fahrenkrug, J.; Wagner, G. Vasoactive Intestinal Polypeptide (VIP) Increases Vaginal Blood Flow and Inhibits Uterine Smooth Muscle Activity in Women. *Eur. J. Clin. Invest.* **1983**, *13*, 321−324. (b) Ottesen, B.; Wagner, G.; Fahrenkrug, J. In *Handbook of Sexology*; Sitsen, J. M. A., Ed.; Elsevier: Amsterdam, 1988; Vol. 6, pp 66−97. (c) Ottesen, B.; Pedersen, B.; Nielsen, J.; Dalgaard, D.; Wagner, G.; Fahrenkrug, J. Vasoactive Intestinal Polypeptide (VIP) Provokes Vaginal Lubrication in Normal Women. *Peptides* **1987**, *8*, 797−800.

(6) Loffler, B.-M. ACE, NEP, ECE-1: Selective and Combined Inhibition. *Curr. Opin. Cardiovasc., Pulm. Renal Invest. Drugs* **1999**, *1*, 352−364.

(7) See for example, (a) De Lombaert, S.; Chatelain, R. E.; Fink, C. A.; Trapani, A. J. Design and Pharmacology of Dual Angiotensin-Converting Enzyme and Neutral Endopeptidase Inhibitors. *Curr. Pharm. Des.* **1996**, *2*, 443−462. (b) Robl, J. A.; Sulsky, R.; Sieber-McMaster, E.; Ryono, D. E.; Cimarusti, M. P.; Simpkins, L. M.; Karanewsky, D. S.; Chao, S.; Asaad, M. M.; Seymour, A. A.; Fox, M.; Smith, P. L.; Trippodo, N. C. Vasopeptidase Inhibitors: Incorporation of Geminal and Spirocyclic Substituted Azepinones in Mercaptoacyl Dipeptides. *J. Med. Chem.* **1999**, *42*, 305−311 and references therein.

(8) McDowell, G.; Nicholls, D. P. The Endopeptidase Inhibitor, Candoxatril, and Its Therapeutic Potential in the Treatment of Chronic Cardiac Failure in Man. *Expert Opin. Invest. Drugs* **1999**, *8*, 79−84.

(9) *Goodman and Gillman's The Pharmacological Basis of Therapeutics*, 10th ed.; Hardman, J., Limbird, L., Eds.; McGraw-Hill Medical Publishing Division: New York, 2001.

(10) Dantzig, A. H. Oral Absorption of β-Lactams by Intestinal Peptide Transport Proteins. *Adv. Drug Delivery Rev.* **1997**, *23*, 63−76.

(11) Devault, A.; Lazure, C.; Nault, C.; Le Moual, H.; Seidah, N. G.; Chretien, M.; Kahn, P.; Powell, J.; Mallet, J.; Beaumont, A.; Roques, B. P.; Crine, P.; Boileau, C. Amino Acid Sequence of Rabbit Kidney Neutral Endopeptidase 24.11 (Enkephalinase) Deduced from a Complementary DNA. *EMBO J.* **1987**, *6*, 1317−1322.

(12) Kerr, M. A.; Kenny, A. J. Purification and Specificity of a Neutral Endopeptidase from Rabbit Kidney Brush Border. *Biochem J.* **1974**, *137*, 477−488.

(13) Oefner, C.; D'Arcy, A.; Henning, M.; Winkler, F. K.; Dale, G. E. Structure of Human Neutral Endopeptidase (Neprilysin) Complexed with Phosphoramidon. *J. Mol. Biol.* **2000**, *296*, 341−349.

(14) (a) Roderick, S. L.; Fournie-Zaluski, M. C.; Roques, B. P.; Matthews, B. W. Thiorphan and Retro-Thiorphan Display Equivalent Interactions When Bound to Crystalline Thermolysin. *Biochemistry* **1989**, *28*, 1493−1497. (b) Matthews, B. W. Structural Basis of the Action of Thermolysin and Related Zinc Peptidases. *Acc. Chem. Res.* **1988**, *21*, 333−340.

(15) Tiraboschi, G.; Jullian, N.; Thery, V.; Antonczak, S.; Fournie-Zaluski, M. C.; Roques, B. P. A Three-Dimensional Construction of the Active Site (Region 507−749) of Human Neutral Endopeptidase (EC.3.4.24.11). *Protein Eng.* **1999**, *12*, 141−149.

(16) For a recent study of thiorphan bound in a human NEP construct see Sahli, S.; Frank, B.; Schweizer, W. B.; Diederich, F.; Blum-Kaelin, D.; Aebi, J. D.; Bohm, H.-J.; Oefner, C; Dale, G. E. Second Generation Inhibitors for the Metalloprotease Neprilysin Based on Bicyclic Heteroaromatic Scaffolds: Synthesis, Biological Activity and X-ray Crystal Structure Analysis. *Helv. Chim. Acta* **2005**, *88*, 731−750.

(17) Holland, D. R.; Barclay, P. L.; Danilewicz, J. C.; Matthews, B. W.; James, K. Inhibition of Thermolysin and Neutral Endopeptidase 24.11 by a Novel Glutaramide Derivative: X-ray Structure Determination of the Thermolysin-Inhibitor Complex. *Biochemistry* **1994**, *33*, 51−56.

(18) Subsequent studies have investigated cocrystal structures of proprietary inhibitors bound in recombinant human NEP. These studies and compound designs derived from them will be disclosed elsewhere.

(19) Challenger, S.; Derrick, A.; Mason, C. P.; Silk, T. Stereoselective Synthesis of a Candoxatril Intermediate via Asymmetric Hydrogenation *Tetrahedron Lett.* **1999**, *40*, 2187−2190.

(20) Barnish, I. T.; James, K.; Terrett, N. K.; Danilewicz, J. C.; Samuels, G. M. R.; Wythes, M. J. Eur. Pat. Appl. EP 274234, 1988.

(21) Maiorana, S.; Pocar, D.; Dalla Croce, P. Studies in the Enamine Field: Reactions of Sulfonyl and Nitro-Enamines with Azides. *Tetrahedron Lett.* **1966**, *48*, 6043−6045.

(22) Viscardi, G.; Savarino, P.; Quagliotto, P.; Barni, E.; Botta, M. Novel Heterocyclic Ligands with Tuned Hydrophobicity. *J. Heterocycl. Chem.* **1996**, *33*, 1195−1200.

(23) Meerwein, H.; Hinz, G. Isomers of 2-Oxypyridine Derivatives. *Justus Liebigs Ann. Chem.* **1930**, *484*, 52−64.

(24) (a) Tadakazu, T.; Keiko, T. Convenient Synthesis of 2,7-Disubstituted 5*H*-1,3,4-Thiadiazolo[3,2-*a*]-Pyrimidin-5-ones and Related Compounds. *Bull. Chem. Soc. Jpn.* **1982**, *55*, 637−638. (b) Steahly, G. W. US Patent 2,422,050, 1947.

(25) Frahm, A. W.; Knupp, G. Asymmetric Synthesis of *cis*-2-Substituted Cyclohexanamines with High Optical Purity. *Tetrahedron Lett.* **1981**, *22*, 2633−2636.

(26) Knupp, G.; Frahm, A. W. Synthesis and Absolute Configuration of 2-Substituted Cyclohexylamine. *Chem. Ber.* **1984**, *117*, 2076−2098.

(27) Medeiros, M. A.; Franca, M. S.; Boileau, G.; Juliano, L.; Carvalho, K. M. Specific Fluorogenic Substrates for Neprilysin (Neutral Endopeptidase, EC 3.4.24.11) which are Highly Resistant to Serine- and Metalloproteases. *Braz. J. Med. Biol. Res.* **1997**, *30*, 1157−1162.

(28) Booth, A. G.; Kenny, A. J. A Rapid Method for the Preparation of Microvilli from Rabbit Kidney. *Biochem. J.* **1974**, *142*, 575−581.

(29) (a) All LogD values were measured at pH 7.4. (b) Stopher, D.; McClean, S. An Improved Method for the Determination of Distribution Coefficients. *J. Pharm. Pharmacol.* **1990**, *42*, 144.

(30) (a) Tanaka, Y.; Fujiwara, T.; Esumi, Y. Sex Difference in the Excretion of Zenarestat in Mice, Rats, Dogs and Humans. *Xenobiotica* **1992**, *22*, 941−947. (b) Terashita, S.; Sawamoto, T.; Deguchi, T.; Tokuma, Y.; Hata, T. Sex-Dependent and Independent Renal Excretion of Nilvadipine Metabolites in Rat: Evidence for a Sex-Dependent Active Secretion in Kidney. *Xenobiotica* **1995**, *25*, 37−47. (c) Hanada, K.; Fujisawa, R.; Kataoka, R.; Nakamura, S.; Ogata, H. Sex-Related Differences in the Renal Disposition of the Acidic Metabolite of Clentiazem in Rats. *Xenobiotica* **2001**, *31*, 725−731.

(31) (a) Kato, Y.; Kuge, K.; Kusuhara, H.; Meier, P. J.; Sugiyama, Y. Gender Difference in the Urinary Excretion of Organic Anions in Rats. *J. Pharmacol. Exp. Ther*. **2002**, *302*, 483−489. (b) Gotoh, Y.; Kato, Y.; Stieger, B.; Meier, P. J.; Sugiyama, Y. Gender Difference in the Oatp1-Mediated Tubular Reabsorption of Estradiol 17β-D-Glucuronide in Rats. *Am. J. Physiol.* **2002**, *282*, E1245−E1254.

(32) Mugford, C. A.; Kedderis, G. L. Sex-Dependent Metabolism of Xenobiotics. *Drug Metab. Rev.* **1998**, *30*, 441−498.

(33) Czerniak, R. Gender-Based Differences in Pharmacokinetics in Laboratory Animal Models. *Int. J. Toxicol.* **2001**, *20*, 161−163.

(34) (a) Munarriz, R.; Kim, S. W.; Kim, N. N.; Abdulmaged, T; Goldstein, I. A Review of the Physiology and Pharmacology of Peripheral Female Genital Arousal in the Animal Model. **2003**, *J. Urol. 170*, S40−S45. (b) Maw, G. N; Wayman, C. P. Eur. Pat. Appl. EP 1097719, 2001. (c) Wayman, C.; Morren, D.; Turner, L.; Van der Graaf, P.; Naylor, A. Inhibition of Neutral Endopeptidase Potentiates Female Genital Blood Flow. *Int. J. Impotence Res.* **2002**, *14*, S7−S8.

JM060133G